Hartree−Fock−Heitler−London Method. 2. First and Second Row Diatomic Hydrides†

Giorgina Corongiu

Dipartimento di Scienze Chimiche ed Ambientali, Università dell'Insubria, Via Lucini 3, I-22100 Como, Italy

Received: June 29, 2006; In Final Form: August 10, 2006

The Hartree−Fock−Heitler−London, HF−HL, method is a new ab initio approach which variationally combines the Hartree−Fock, HF, and the Heitler−London, HL, approximations, yielding correct dissociation products. Furthermore, the new method accounts for nondynamical correlation and explicitly considers avoided crossing. With the HF−HL model we compute the ground-state potential energy curves for H_2 [$^1\Sigma_g^+$], LiH [$X\ ^1\Sigma^+$], BeH [$^2\Sigma^+$], BH [$^1\Sigma^+$], CH [$^2\Pi$], NH [$^3\Sigma^-$], OH [$^2\Pi$], and FH [$^1\Sigma^+$], obtaining in average 80% of the experimental binding energy with a correct representation of bond breaking. Inclusion of ionic configurations improves the computed binding energy. The computed dipole moment is in agreement with laboratory data. The dynamical and nondynamical correlation energies for atomic and molecular systems with 2−10 electrons are analyzed. For BeH the avoided crossing of the two lowest [$^2\Sigma^+$] states is considered in detail. The HF−HL function is proposed as the *zero-order* reference wave function for molecular systems. To account for the dynamical correlation energy a post-HF−HL technique based on multiconfiguration expansions is presented. We have computed the potential energy curves for H_2 [$^1\Sigma_g^+$], HeH [$^2\Sigma^+$], LiH [$X^1\Sigma^+$], LiH [$A^1\Sigma^+$], and BeH [$^2\Sigma^+$]. The corresponding computed binding energies are 109.26 (109.48), 0.01 (0.01), 57.68 (58.00), 24.19 (24.82), and 49.61 (49.83) kcal/mol, with the experimental values given in parentheses. The corresponding total energies are −1.1741, −3.4035, −8.0695, −7.9446, and −15.2452 hartrees, respectively, the best ab initio variational published calculations, H_2 excluded.

1. Introduction

It is well-known that, at the beginning of quantum chemistry, two approaches were predominant in the attempts to explain, with quantum theory, the forces responsible for holding atoms together as a molecule. These were the linear combination of atomic orbitals−molecular orbitals[1−3] (LCAO-MO) and the Heitler−London[4] (HL). The two approximations represent two different implementations of a one-particle model. In time these techniques evolved into the analytical Hartree−Fock (HF)[5,6] approximation (at the time a most promising method for atomic systems[7−9]) and the valence bond (VB) approximation.[10−15] Since the LCAO-MO and the HL offered only reasonable, but not sufficiently reliable, approximations, the past 5 decades have seen a strong effort aimed at more accurate quantum mechanical solutions often starting from the two original approximations. The introduction of perturbation methods with Møller and Plesset[16] opened new avenues[17,18] complementing the variational approaches**;** recently the second-order perturbation theory has been utilized in the CASPT2 method.[19]

We hasten to call to mind that today there are different and appealing alternatives to the approaches mentioned above. Relatively recent publications[20,21] present in detail the evolution and the present status of quantum chemistry. Today, the methodological effort continues with attempts to extend the applicability of ab initio methods to larger systems and with proposals of increasingly reliable semiempirical methods.[22−25]

Hereafter, the designation HF is used to indicate the restricted Hartree−Fock method, but later in this work we shall expand its definition to the complete Hartree−Fock,[9] a particular multiconfiguration expansion yielding nondynamical correlation in atoms. In this paper the designation HL wave function is restricted to HL type wave functions which dissociate into HF atoms in the lowest electronic state. This restriction is introduced to provide a unique definition for the HL functions designed to facilitate comparison with HF functions.

From a conceptual point of view the pragmatic rush to develop new techniques and methods has understandably left numerous gaps. In addition, in the early days the enthusiasm and a highly competitive atmosphere in the new field of computational chemistry highlighted the differences rather than the complementary nature of the two traditional and competing quantum chemical approaches. Today, we can afford a more relaxed attitude.

As we all know, the computation of the electronic correlation energy,[26,27] E_c, is the goal of any post-Hartree−Fock approach. Hylleraas'[28] direct use of interelectronic distances in the wave function and Hartree et al.'s[9] elimination of near-degeneracy effects with short multiconfiguration (MC) expansions were among the very early attempts to deal with the correlation energy problem.

In a few situations the two quantum chemical models, HF and HL, fail to provide a theory capable of predicting (even qualitatively) the forces responsible for holding together atoms in a molecule. It follows that neither one of the two models can be chosen as a general zero-order approximation for quantum chemistry, namely, a "reference function" which qualitatively approximates laboratory data with consistency and with equal accuracy at any internuclear separation.

In this work, following the introductory proposal of ref 29, we variationally combine HF and HL models yielding the

† Work partially presented at the XII ICQC Meeting, Kyoto, Japan, May 2006.

10.1021/jp064065l CCC: $33.50
Published on Web 09/21/2006

Hartree−Fock−Heitler−London model, HF−HL, detailed in section 2. The latter is proposed at two accuracy levels: the HF−HL level, which accounts for the nondynamical correlation corrections, and the post-HF−HL level, which also accounts for the dynamical correlation: this partitioning of the correlation energy corrections in the context of the HF−HL model is discussed in section 3.

2. HF−HL Computational Method

Recall that the HF method fails to reproduce bond breaking, even qualitatively. On other occasions the method fails to predict binding for molecules with known strong laboratory binding energy. Furthermore, avoided state crossing, a rather frequent molecular event, is ignored. On the other hand, the method applies self-consistently the variational principle to a selected electronic configuration, starting with simple trial functions, and utilizes a robust algorithm constrained, however, by the basis set choice (the latter must be adequate to avoid basis set superposition errors, BSSE).

The HL method at dissociation builds the molecular wave function with functions representing the separated neutral atoms, with spin and angular momentum selected to ensure correct dissociation products.[3] In this work, the HL function at dissociation is limited to neutral atomic ground states represented either with HF functions or with more accurate approximations, such as configuration interaction,[30] CI, or MC expansions; for the latter in this study we use the Dalton computational code.[31]

Since in the HF−HL model we combine the HF and the HL functions, we consider the Hartree−Fock atoms as reasonable first-order approximations to represent the HL atomic dissociation products. However, when we consider more accurate wave functions for the HL (or for the HF) model, the HF (or HL) component of the HF−HL linear combination is equivalently improved, to ensure a "balanced HF−HL representation.

An important assumption of the HF−HL method is that the total molecular correlation energy can be partitioned for example into the sum of the correlation energy of the separated atoms and correlation contributions arising from the new electron pairs and electronic charge rearrangements concomitant with the molecular formation process (namely, the "molecular extracorrelation energy"[32]). The particular decomposition of the correlation energy adopted in the HF−HL model is exposed in detail in section 3.

The HF−HL approach is proposed as a three-step process with increasing accuracy at each successive step. This work is mainly concerned with the first step presented in section 2.1. In section 2.2 we present a post-HF−HL algorithm (HF−HL steps 2 and 3) to obtain the dynamical correlation correction.

2.1. First Step: the HF−HL Model. In the first HF−HL step we variationally combine the HF and the HL functions, the latter being built with HF atoms,[29] thus obtaining by construction correct dissociation products. Further the HF and HL approximations are improved with short MC expansions, to introduce near-degeneracy correlation energy (for details, see section 3). Finally, if the state in consideration results from an avoided potential energy curve crossing, then both states participating in the crossing are explicitly considered. In this way we account for the nondynamical correlation in the HF−HL function.

Formally, we start by defining with obvious notation the HF, Ψ_{HF}, and the HL, Ψ_{HL}, functions given in eqs 1 and 2, respectively:

$$\Psi_{HF} = \det(\Phi_1, ..., \Phi_i, ..., \Phi_n) \quad (1)$$

$$\Psi_{HL} = \sum_k \det(\varphi_{1k}, .., \varphi_{ik}, ..., \varphi_{mk}) \quad (2)$$

Above, Φ_i refers to the ith HF molecular orbital and φ_{lk} to the lth atomic orbital of the kth determinant in the HL function. Note that the HL functions are constructed to satisfy the correct spin coupling constraints.[33]

When at dissociation the atoms in the molecule are in a state with near-degeneracy, and/or when there is avoided crossing, then in eqs 1 and 2 the Ψ_{HF} and the Ψ_{HL} are replaced by very short MC expansions to account for near-degeneracy and avoided crossing.

The HF−HL wave function ψ''_{HF-HL} is obtained by determining variationally the linear combination

$$\Psi''_{HF-HL} = c_1\Psi'_{HF} + c_2\Psi'_{HL} \quad (3)$$

where with the notation Ψ'_{HF} and Ψ'_{HL} we indicate either standard HF and HL functions or very short MC−HF and MC−HL expansions, when there is near degeneracy and/or avoided states crossing; in section 3 we shall introduce a specific notation to avoid ambiguities.

In eq 3 the c_1 and c_2 coefficients are obtained variationally by solving the equation $\mathbf{(H - SE)C} = 0$ with **H** and **S** the interaction supermatrixes containing the Hamiltonian and the overlap matrix elements, respectively. The Φ_i orbitals of Ψ'_{HF} are a linear combination of a basis set of Gaussian functions, and the same basis set is also used to expand the orbital φ_{lk} of Ψ'_{HL}. We recall that the Φ_i orbitals form an orthogonal set, whereas the φ_{lk} orbitals can be nonorthogonal. For the latter case, following Löwdin[34] the interaction between two determinants, d_a and d_b, is given by

$$\langle d_a|H|d_b\rangle = \sum_{ij} h_{ij}S^{(i,j)} + \sum_{i<k,j<l} [\langle ij|kl\rangle - \langle il|kj\rangle]S^{(i,k,j,l)} \quad (4)$$

where the indices i and k refer to the occupied orbitals of d_a and j and l to those of d_b; $S^{(i,j)}$ and $S^{(i,k,j,l)}$ are the first- and second-order cofactors of the overlap matrix **S**, constructed with the occupied orbitals of d_a and d_b. The cofactors are computed with the algorithm proposed in ref 35, adapting routines from the public domain Linpack library.[36]

In eq 3 we have not included ionic structures in the HL component, since it would account for a fraction of the total dynamical correlation, a task left for the post-HF−HL approach. However, for the hydrogen fluoride molecule (section 10) we have added two ionic structures[37] obtaining a notable gain in the computed binding energy.

2.2. Post HF−HL. Since both the HF and the HL methods can be extended in order to include dynamical correlation, the equivalent feasibility exists for the HF−HL method. Keeping in mind the decomposition of dynamical correlation energy into two components, namely, a molecular component (the molecular extra correlation) and a second one resulting from the sum of the dynamical correlation energy of the separated atoms (see section 3), we envision two steps in the post HF−HL method.

The dynamical molecular extra correlation energy is computed in the second HF−HL step (to obtain accurate binding energies) and the atomic dynamical correlation in the third step (to obtain accurate total energies). The correlation techniques adopted in the second and third steps are MC expansions complementing each other. Thus, presently, the post-HF−HL method makes

use—with variants—of avenues tested in post-Hartree−Fock computations.

In the post-HF−HL method, the dynamical correlation correction is introduced by replacing in eq 3 the Ψ'_{HF} function with an extended MC−HF linear expansion of HF-type functions, $\Sigma_p a_p \Psi_{p(HF)}$, and Ψ'_{HL} with an MC−HL expansion of HL-type functions, $\Sigma_q b_q \Psi_{q(HL)}$:

$$\Psi'_{HF-HL} = \sum_p a_p \Psi_{p(HF)} + \sum_q b_q \Psi_{q(HL)} \quad (5)$$

The p, q indices define excited configurations in the MC expansions, and a_p, b_q, are the corresponding variational expansion coefficients. The two MC expansions complement each other. Equation 5 constitutes the second HF−HL step.

The remaining dynamical correlation energy is computed by solving eq 6, the third step of the HF−HL approach:

$$\Psi_{HF-HL} = \sum_P a_P \Psi_{P(HF)} + \left[\sum_q b_q \Psi_{q(HL)} + \sum_r b'_r \Psi_{r(HL)} \right] \quad (6)$$

In eq 6 the index P replaces the p of eq 5 to indicate a new and more extended expansion. For the HL component we use two MC−HL linear expansions, one $\Sigma_q b_q \Psi_q$ (present in eq 5) with optimized atomic orbitals, the second $\Sigma_r b'_r \Psi_r$ (generally an extended expansion) constructed by adapting MC−HF functions originally computed for the separated atoms. The latter can be determined once and for all and can be used over and over for different molecules in HF−HL computations containing atoms with the same Z number and state specification, thus transferable from molecule to molecule, as exemplified by the HF−HL computations on the LiH and Li_2 molecules.[29]

For very few electron systems the dynamical correlation can be obtained with the first term of eq 5, namely, via CI or CASSCF computations. For polyatomic systems the transferability of $\Sigma_r b'_r \Psi_{r(HL)}$ becomes more and more important the larger the system. The computation[29] of LiH and Li_2 provides an initial example (additional work is in progress).

Recall that in the post-HF−HL method the dynamical correlation can be introduced with a variety of alternative techniques either ab initio or semiempirically.[29,38] The extensive computations by Lie and Clementi for diatomic homopolar molecules[39] and hydrides[40] have clearly shown that density functional corrections applied to short MC expansions (used to correct the HF function near dissociation) yield most reasonable binding and total energies. Note that for HF−HL functions the correct dissociation is ensured by construction; thus, the available and tested semiempirical density functionals[38−40] can be used to deal with the dynamical correlation.

3. Dynamical and Nondynamical Correlation Energy in the HF−HL Model

The standard definition of the correlation energy relates to the HF method. Therefore, we need more general definitions for the correlation energy, an appropriate notation and a detailed description on the specific partitioning of the correlation energy adopted in the HF−HL model.

Since molecules are systems of nuclei and electrons, the correlation energy can be defined with reference to an expansion into one-, two-, ..., many-electron energies obtained by solving the corresponding one-, two-, ..., many-electron exact solutions. The approximated solution from a given nonrelativistic model (like HF, HL, and HF−HL) brings about energy differences relative to the energies obtained (a) with the exact one-electron nonrelativistic model, difference called nondynamical correlation, E_c(nondyn), and (b) with the exact many-electron nonrelativistic model, the total correlation energy, E_c. The difference between the total and the nondynamical correlation energies is the dynamical correlation energy E_c(dyn).

However, if we stress the viewpoint that molecules are composed of atoms, then the correlation energy can be broken down into two components: one, $\Sigma_a \epsilon_a$, for the sum of the correlation corrections for the separated atoms and the second, η_M, for the molecular extracorrelation energy. The two viewpoints are complementary and therefore the partitioning of the correlation energy is also complementary.

The nondynamical correlation errors in the HF model are due to (1) neglect of near-degeneracy, (2) the constraint of doubly orbital occupancy for molecular systems near dissociation, and (3) neglect of avoided curve crossing.

We consider near-degeneracy. The nondynamical correlation has been taken into account by Hartree et al.[9] with short MC expansions of the near-degenerate configurations. Later, a different approach based on perturbation methods was proposed first by Sinanoglu[41,42] and later by others.[43−45] Following Hartree at al.,[9] Veillard and Clementi[46] computed, with Slater-type functions, the nondynamical correlation in the second row atoms and ions using MC expansions of two configurations—$1s^2 2s^2 2p^n$ and the nearly degenerate $1s^2 2s^0 2p^{n+2}$.

We have recomputed, with the Gaussian basis set defined in section 4, the near-degeneracy energy correction for the ground state of the Be [^{1}S], B [^{2}P], and C [^{3}P] atoms, obtaining the following nondynamical correlation energies: 0.043 72, 0.034 81, and 0.019 36 hartree, respectively, in substantial agreement with the computation by Veillard and Clementi.[46] In the MC expansion the coefficients of the near-degenerate configuration $1s^2 2s^0 2p^{n+2}$ are 0.25, 0.17, and 0.15 for Be, B, and C, respectively. A relatively small amount of mixing is sufficient to remove near-degeneracy errors in atoms and, as shown in section 9, also in molecules.

Concerning the constraint of doubly orbital occupancy, we recall that the HF model approaching dissociation can become unstable, leading to grossly incorrect energies. The use of the unrestricted HF algorithm avoids this catastrophic behavior, but the resulting wave function is incorrect. The alternative, proposed by Lie and Clementi[39,40] is of difficult implementation for molecule larger than diatomic, particularly for multiple bonds. For example, even in the ground state of N_2 10 configurations are needed to obtain correct dissociation[39] to be compared to only two configurations (one from HF and one from HL) in the HF−HL model, where the correct dissociation is obtained by construction.

The third source of nondynamical correlation is related to the degeneracy at the crossing of states with the same symmetry—a situation very common in excited states, but also frequently present in ground states,[3] as in, for example, BeH (see section 7).

In the HL approximation, the nondynamical correlation error is due (1) to the neglect of near-degeneracy, (2) to the constrained selection of the lowest atomic state at dissociation, and (3) to the neglect of avoided state crossing.

In summary, we partition E_c as

$$E_c = \sum_a \epsilon_a + \eta_M \quad (7)$$

Further, we distinguish $E_{c(HF)}$ from $E_{c(HL)}$, since the correlation

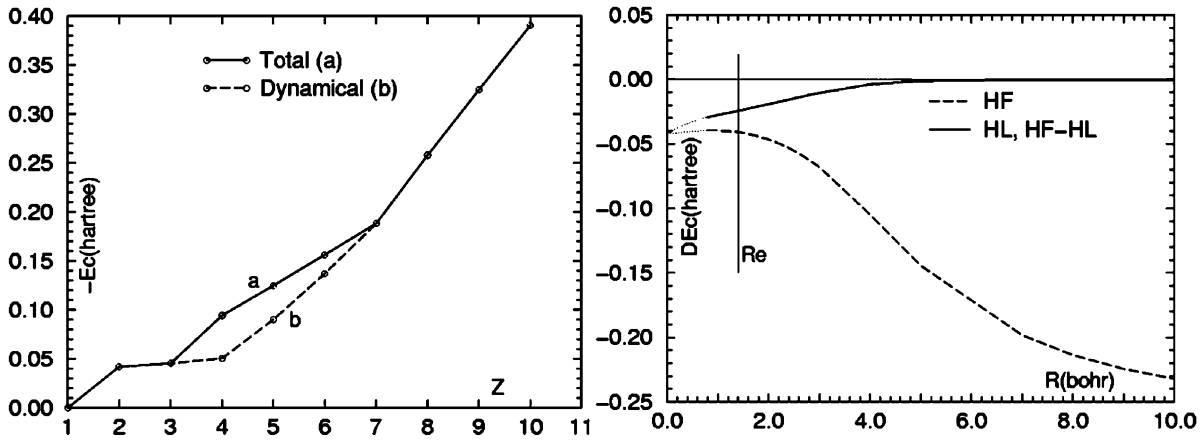

Figure 1. Nondynamical correlation. Left: first and second row ground-state atomic correlation energy with and without near-degeneracy correction. Right: correlation energy for H_2 from Hartree−Fock, Heitler−London, and Hartree−Fock−Heitler−London.

TABLE 1: Laboratory Molecular Binding Energy (kcal/mol), E_b, Laboratory Equilibrium Distance (bohr), R_e, Total Nonrelativistic Energy at Equilibrium, $E_T(R_e)$, and at Dissociation, $E_T(R_\infty)$, Atomic HF Energies (hartrees), E_{HF} (Limit), and E_{HF} (This Work)

molecule	E_b[a]	R_e[a]	$E_T(R_e)$	$E_T(R_\infty)$	E_{HF} (limit)		E_{HF} (this work)
H_2 [$^1\Sigma_g^+$]	109.48[b]	1.4[b]	−1.174 4757	−1.000 000	H [^{2}S]	−0.500 000	-0.499999
HeH [$^2\Sigma^+$]	0.01[c]	7.00	−3.403 7459	−3.403 7243	He [^{1}S]	−2.861 680	-2.861679
LiH [$^1\Sigma^+$]	58.00	3.0150	-8.070 491	−7.978 062	Li [^{2}S]	−7.432 727	-7.432721
BeH [$^2\Sigma^+$]	49.83[d]	2.5371	−15.246 772	−15.167 363	Be [^{1}S]	−14.573 023	-14.573016
BH [$^1\Sigma^+$]	84.1[e]	2.3289	−25.287 95	−25.153 93	B [^{2}P]	−24.529 061	-24.529036
CH [$^2\Pi$]	83.9	2.1163	−38.478 69	−38.344 99	C [^{3}P]	−37.688 619	-37.688616
NH [$^3\Sigma^-$]	80.5[f]	1.9582	−55.217 54	−55.089 25	N [^{4}S]	−54.400 934	-54.400924
OH [$^2\Pi$]	106.6	1.8324	−75.737 08	−75.567 2	O [^{3}P]	−74.809 398	-74.809384
FH [$^1\Sigma^+$]	141.5[g]	1.7325	−100.459 2	−100.233 7	F [^{2}P]	−99.409 349	-99.409343

[a] Reference 47. [b] Reference 48. [c] Reference 49. [d] Reference 50. [e] Reference 51. [f] Reference 52. [g] Reference 53.

energy is an error specific for a given model, and write

$$E_{c(HF)} = \sum_a \epsilon_{a(HF)}(\text{nondyn}) + \sum_a \epsilon_{a(HF)}(\text{dyn}) + \eta_{M(HF)}(\text{nondyn}) + \eta_{M(HF)}(\text{dyn}) \quad (8a)$$

$$E_{c(HL)} = \sum_a \epsilon_{a(HL)}(\text{nondyn}) + \sum_a \epsilon_{a(HL)}(\text{dyn}) + \eta_{M(HL)}(\text{nondyn}) + \eta_{M(HL)}(\text{dyn}) \quad (8b)$$

For the HF−HL method $\Sigma_a \epsilon_a$(nondyn) is taken into account by including near-degeneracy and avoided crossing and η_M(nondyn) by ensuring correct dissociation: thus for the HF−HL model the correlation is reduced to

$$E_{c(HF-HL)} = \eta_{M(HF-HL)}(\text{dyn}) + \sum_a \epsilon_{a(HF-HL)}(\text{dyn}) \quad (9)$$

We now introduce definitions and a specific notation needed to ensure a coherent discussion in the following of this work. We indicate as MC−HF and MC−HL multiconfiguration expansions of HF type and HL type functions, respectively. When needed, we use the specific notation HF(n), HL(m), and HF−HL(n,m) to designate MC−HF expansions of n configurations, MC−HL expansions of m configurations, and HF−HL function composed by the linear combination of HF(n) and HL(m). The energies $E_{HF}(n)$, $E_{HL}(m)$, and $E_{HF-HL}(n,m)$ correspond to the wave functions HF(n), HL(m), and HF−HL(n,m), respectively. Equivalent notation is used for the computed binding energies, E_b, and the correlation energies, E_c. To indicate a specific electronic configuration within a given MC expansion, we use the notation HF-n, HL-m.

We indicate the HF(n), HL(m), and HF−HL(n,m) correlation energies as $E_{c(HF)}(n)$, $E_{c(HL)}(m)$, $E_{c(HF-HL)}(n,m)$; these are defined as the energy difference between $E_{HF}(n)$, $E_{HL}(m)$, $E_{HF-HL}(n,m)$ and the exact nonrelativistic energy.

In Figure 1 we report two examples to typify the nondynamical correlation energy. In the left inset we present the correlation energy for atoms with and without near-degeneracy. The dashed line denotes the dynamical correlation energy obtained by subtracting from the total correlation the near-degenerate correlation energy of Be, B, and C. In the right inset, we report the correlation energy from the HF, the HL, and the HF−HL models in H_2 [$^1\Sigma_g^+$]. The usual definition of correlation energy related to the HF model is clearly unsatisfactory, since, at dissociation, the correlation energy of H_2 should vanish. For the HF−HL model the correlation energy of H_2 is reduced to the dynamical component (see eq 9). In the inset the dotted lines are interpolations from short H_2 internuclear distance values to the united atom, He [^{1}S].

4. HF−HL Method for First- and Second-Period Monohydrides

In this work we stress the HF−HL approach, since we are searching for a reference function for molecular computation. We consider as a test case the first and second row diatomic hydrides. In Table 1 we list laboratory binding energies,[47−53] E_b, equilibrium internuclear distances, R_e, and "exact" nonrelativistic energies at equilibrium, $E_T(R_e)$, and at dissociation, $E_T(R_\infty)$, obtained from recent tabulations of atomic energies[54] and the numerical HF energy limit for atoms[55] very close to previous analytical HF computations.[56] $E_T(R_e)$ is obtained by adding the laboratory binding energy to $E_T(R_\infty)$, the "exact" nonrelativistic

energy of the separated atoms.[54] For the molecules considered here and for the accuracy at which we are aiming (0.001 hartree) the relativistic contribution to the molecular binding is negligible, even when the relativistic atomic correction[57] is comparable to the molecular binding energy. For example, for H_2O at equilibrium geometry the relativistic correction[58] to the binding energy is −0.000 582 hartrees. However, we recall that at $Z = 13$ the atomic correlation energy and the relativistic correction are nearly equal in value.

We used the following basis sets: for the H atom [10,5,4,/6,5,4] in the hydrides and [10,5,4,4] in the H_2 and HeH molecules; for the He atom [14,9,8,5,2]; for the Li atom [15,-10,6,1/10,8,6,1]; for the Be atom [17,8,6,3/11,8,6,3]; for the B atom [15,11,7,5/9,8,6,4]; for the C atom [17,13,6,5/11,8,5,4]; for the N and O atoms [17,13,5,4/9,7,5,4], and for the F atom [18,13,5,4/12,6,5,4]. These basis sets yield the Hartree−Fock atomic ground-state energies given in Table 1.

We have tested our proposal by comparing laboratory and computer data for diatomic hydrides in the HF, HL, and HF−HL models. Data from a large number of potential energy curves are analyzed. For each potential curve we compute the energy at 30−40 internuclear distances, stressing equally short and large internuclear distances, the latter essential for understanding the formation and breaking of bonds. Note that in the figures throughout this paper the marks (circles, diamonds, and triangles, etc.) on the potential energy curves indicate internuclear distances for which a computation has been carried out. In addition, in a given inset all curves are obtained with the same number of computed points (but in a given inset the marks might only be given on one curve).

In this work we search for a method that is (a) equally valid in the full range of internuclear separations from near equilibrium to dissociation, (b) valid for ground and excited states, (c) computationally easy, (d) of immediate physical interpretability, (e) more accurate than the HF and HL approximations, and (f) easily extendable to higher accuracy, leading eventually to exact wave functions. We have listed above the general characterization of a molecular "reference function". In this work we prove that the HF−HL function fulfills all the criteria listed above. The search for a proper reference function is not a new topic in quantum chemistry. We refer, for example, to papers by Lie and Clementi,[39,40] Fritsche,[59] and Valderrama et al.[60]

We recall that the most accurate computations for the second row hydrides are the quantum Monte Carlo,[61] QMC, limited to the experimental equilibrium internuclear distance.

In Table 2 we provide the electronic configuration of the HF and HL functions needed in the HF−HL computation of monohydrides. To introduce near-degeneracy correlation, we have to consider more than one dissociation product and, therefore, more than one set of HF and HL configurations. The same holds true for state crossing. For the HF type functions the characterization is provided by the molecular orbital electronic configuration. For the HL method we specify the atomic states used to construct the Heitler−London function at dissociation followed by the list of the spin pairs. For example, for LiH [$^1\Sigma^+$] we give the two atomic states at dissociation H [^{2}S] and Li [^{2}S], the corresponding electronic configurations $(1s^1)_H$ and $(1s^22s^1)_{Li}$ and the spin pair $1s_H2s_{Li}$. For the XH hydrides considered here, the lowest doubly occupied orbital, $1\sigma^2$ (HF language) and the $1s^2_X$ electron pair of the X atom (HL language), is not reported, since it is tacitly understood to be present.

TABLE 2: Hydrides: Characterization for Hartree−Fock and Heitler−London Functions

case	Hartree-Fock configuration	Heitler-London diss. & pairs
LiH [$^1\Sigma^+$]	HF-1: $2\sigma^2$	H [^{2}S] Li [^{2}S]: $(1s^1)_H\,(1s^22s^1)_{Li}$ $\rightarrow 1s_H\,2s_{Li}$
BeH [$^2\Sigma^+$]	HF-1: $2\sigma^2\,3\sigma^1$ HF-2: $2\sigma^03\sigma^11\pi^2$ HF-3: $2\sigma^1\,3\sigma^14\sigma^1$	H [^{2}S] Be [^{1}S]: $(1s^1)_H\,(1s^22s^2)_{Be}$ $\rightarrow 2s_{Be}2s_{Be}$ $\rightarrow 1s_H$ H [^{2}S] Be [^{1}S]: $(1s^1)_H\,(1s^22p^2)_{Be}$ $\rightarrow 2p_{Be}2p_{Be}$ $\rightarrow 1s_H$ H [^{2}S] Be [^{3}P]: $(1s^1)_H\,(1s^22s^12p^1)_{Be}$ $\rightarrow 1s_H2p_{Be}$ $\rightarrow 2s_{Be}$
BH [$^1\Sigma^+$]	HF-1: $2\sigma^2\,3\sigma^2$ HF-2: $2\sigma^0\,3\sigma^2\,1\pi^2$ HF-3: $2\sigma^1\,3\sigma^2\,1\pi^1$ HF-4: $2\sigma^2\,3\sigma^14\sigma^1$	H [^{2}S] B [^{2}P]: $(1s^1)_H\,(1s^22s^22p^1)_B$ $\rightarrow 2s_B2s_B$ $\rightarrow 1s_H2p_B$ H [^{2}S] B [^{2}P]: $(1s^1)_H\,(1s^22p^3)_B$ $\rightarrow 2p_B2p_B$ $\rightarrow 1s_H2p_B$ H [^{2}S] B [^{2}P]: $(1s^1)_H\,(1s^22s^12p^2)_B$ $\rightarrow 2p_B2p_B$ $\rightarrow 1s_H2s_B$
CH [$^2\Pi$]	HF-1: $2\sigma^2\,3\sigma^21\pi^1$ HF-2: $2\sigma^0\,3\sigma^21\pi^3$ HF-3: $2\sigma^1\,3\sigma^21\pi^2$ HF-4: $2\sigma^2\,3\sigma^14\sigma^11\pi^1$	H [^{2}S] C [^{3}P]: $(1s^1)_H\,(1s^22s^22p^2)$ $\rightarrow 2s_C2s_C$ $\rightarrow 1s_H2p_C$ $\rightarrow 2p_C$ H [^{2}S] C [^{3}P]: $(1s^1)_H\,(1s^22p^4)_C$ $\rightarrow 2p_C2p_C$ $\rightarrow 1s_H2p_C$ $\rightarrow 2p_C$ H [^{2}S] C [^{3}P]:$(1s^1)_H\,(1s^22s^12p^3)_c$ $\rightarrow 2p_c2p_c$ $\rightarrow 1s_H2s_C$ $\rightarrow 2p_C$
NH [$^3\Sigma^-$]	HF-1: $2\sigma^2\,3\sigma^2\,1\pi^2$	H [^{2}S] N [^{4}S]:$(1s^1)_H\,(1s^22s^22p^3)_N$ $\rightarrow 2s_N2s_N$ $\rightarrow 1s_H2p_N$ $\rightarrow 2p_N$ $\rightarrow 2p_N$
OH [$^2\Pi$]	HF-1: $2\sigma^2\,3\sigma^2\,1\pi^3$	H [^{2}S] O [^{3}P]: $(1s^1)_H\,(1s^22s^22p^4)_O$ $\rightarrow 2s_O2s_O$ $\rightarrow 2p_O2p_O$ $\rightarrow 1s_H\,2p_O$ $\rightarrow 2p_O$
HF [$^1\Sigma^+$]	HF-1: $2\sigma^2\,3\sigma^2\,1\pi^4$	H [^{2}S] F [^{2}P]: $(1s^1)_H\,(1s^22s^22p^5)_F$ $\rightarrow 2s_F2s_F$ $\rightarrow 2p_F2p_F$ $\rightarrow 2p_F2p_F$ $\rightarrow 1s_H\,2p_F$

5. H_2 [$^1\Sigma_g^+$] and HeH [$^1\Sigma^+$] Ground States

In this section we report on computations with the post-HF−HL method for the H_2 [$^1\Sigma_g^+$] and HeH [$^2\Sigma^+$] ground state (see ref 29 for preliminary computations).

The basis sets we have selected for this work are sufficiently extended for HF, HL, and HF−HL computations, but likely fall short for computations with accuracy superior to our threshold of 0.001 hartrees. For very accurate computations we refer for H_2 [$^1\Sigma_g^+$] to Kolos et al.,[48] and to QMC data[62] for HeH [$^2\Sigma^+$].

In the top left inset of Figure 2 we report the H_2 [$^1\Sigma_g^+$] ground-state potential energy curves for the HF, HL, and HF−HL approximations. In this work we have extended our previous basis set[29] by uncontracting the s functions and by adding four 4f Gaussian functions. The new binding energy is 109.26 kcal/mol, which can be compared to the previous value[29] of 108.56 kcal/mol and to the exact value of 109.48 kcal/mol. We postpone analyses of the computed data to the end of the paper, where we compare the entire set of computed hydrides (section 11).

The HeH [$^2\Sigma^+$] molecule is included in this work to provide data for a three-electron diatomic hydride, thus, completing our study on diatomic hydrides from 2 to 10 electrons. The HeH [$^2\Sigma^+$] molecule has one of the weakest bonds in chemistry (even among van der Waals bonds) in the range 0.000 0215−0.000 0227 hartrees[49] in agreement with QMC computations,[62]

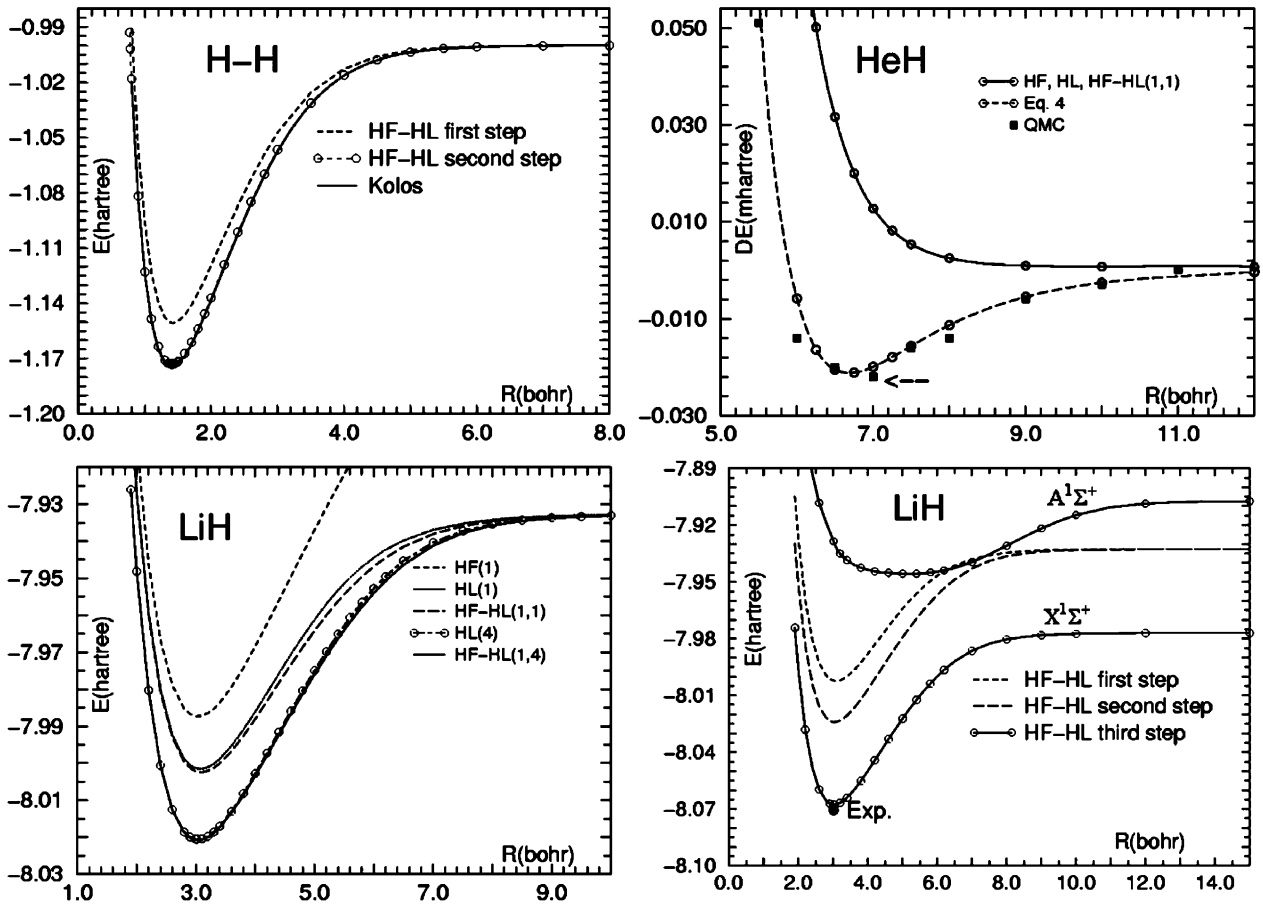

Figure 2. Potential energies from HF, HL, and HF−HL models for H_2 [$^1\Sigma_g^+$] (top left panel), for HeH [$^2\Sigma^+$] (top right panel; square marks are for QMC computations,[55] and the arrow indicates the experimental value[31]). Potential energies from HF, HL, and HF−HL for LiH [$X^1\Sigma^+$] (bottom left panel), HF−HL from first, second, and third steps for LiH [$X^1\Sigma^+$] and LiH [$A^1\Sigma^+$] (bottom right panel).

yielding 0.000 0216 hartrees. In the top right inset of Figure 2 we report the HF, HL, and the "simple" HF−HL computations, yielding essentially three indistinguishable repulsive curves. Post-HF−HL computations and the QMC results,[62] the latter indicated by square marks, are also reported in the inset. For HeH [$^2\Sigma^+$] the MC expansion (eq 5) yields a binding energy of 0.000 0211 hartrees, which is in agreement with experimental data. The total energies computed at the equilibrium distance for HF, HL, and HF−HL are essentially equal in value and amount to −3.361 6665 hartrees (−3.361 6793 hartrees at dissociation); for the post-HF−HL computation the computed energy is −3.403 4746 hartrees (−3.403 4535 hartrees at dissociation). The correlation energy for the HF, HL, and HF−HL function amounts to −0.041 646 hartrees, essentially the He [^{1}S] value.

6. [$X^1\Sigma^+$] and [$A^1\Sigma^+$] States for LiH

The LiH [$X^1\Sigma^+$] dissociates into Li [^{2}S] and H [^{2}S] and the [$A^1\Sigma^+$] state dissociates into in Li [^{2}P] and H [^{2}S]. The LiH [$^1\Sigma^+$] ground-state potential energy curves are reported in the bottom left inset of Figure 2 for the HF, HL, and HF−HL approximations. The HF, HL, and HF−HL curves yield at the equilibrium distance a molecular binding energy of 34.27, 43.11, and 43.66 kcal/mol and a total molecular energy of −7.987 34, −8.001 42, and −8.002 30 hartrees, respectively.

To exemplify the energy gains, one can obtain with relatively short MC−HL expansions of $\Sigma_q b_q \psi_{q(\mathrm{HL})}$ type, we have performed computations with a four-configuration optimized MC−HL function (three σ and one π) obtaining a binding energy of 55.25 kcal/mol (see curve HF−HL(1,4) in the bottom left inset of Figure 2).

In the bottom right inset of Figure 2 we compare the potential energies computed with the HF−HL approximation and with post-HF−HL second and third steps. Concerning the second step we obtain at $R = 3.015$ bohr a binding energy of 57.32 kcal/mol (the experimental value is 58.00 kcal/mol) and a total energy of −8.024 07 hartrees, −7.932 72 hartrees at dissociation.

The third step adds inner shell correlation. For this step we add to the HF function of the second step an HL component resulting from two MC−HL expansions, $\Sigma_q b_q \psi_{q(\mathrm{HL})}$ and $\Sigma_r b'_r \psi_{r(\mathrm{HL})}$ of eq 6. The first expansion contains four configurations, and we have considered 2444 terms in the second, since from this computation we obtain also the first excited state discussed below. For the ground state the binding energy is 56.83 kcal/mol, the total energy at equilibrium is −8.067 63 and −7.977 07 hartrees at dissociation (see bottom left inset of Figure 2) not far from the exact energies of Table 1. Note that the loss of 0.5 kcal/mol in the third step binding energy relative to the second step, implies that the inner shell correlation is more accurately accounted for in the Li atom (LiH at dissociation) than in the LiH molecule at equilibrium. This calls for an extension of the MC−HL expansion of $\Sigma_q b_q \psi_{q(\mathrm{HL})}$ type and then eventual improvements in the remaining MC expansions. However, first of all we must examine our basis set ability to yield inner shell correlation energy.

For the systems listed in Table 3, we have performed HF and CASSCF computations, with all the available orbitals in the active space. Therefore the total energies are equal to those

TABLE 3: HF and CASSCF Data for LiH and BeH and Related Species

index	system	R (bohr)	$-E_{HF}$ (hartrees)	$-E_{CASSCF}$ (hartrees)	$-E_{corr.}$ (hartrees)
a	Li [^{2}S]		7.432 72	7.477 08	0.044 36
b	Li [^{2}P]		7.365 04	7.409 11	0.044 07
c	Li^+ [^{1}S]		7.236 41	7.278 98	0.042 57
d	LiH [X $^1\Sigma^+$]	3.015	7.987 34	8.068 89	0.081 55
e	LiH [X $^1\Sigma^+$]	40.00	7.932 72	7.977 09	0.044 37
f	LiH [X $^1\Sigma^+$][a]	3.015	7.987 34	8.024 07	0.044 82
g	LiH^{2+} [$^1\Sigma$]	3.015	6.906 02	6.948 62	0.042 60
h	LiH^{2+} [$^1\Sigma$]	40.00	7.211 41	7.253 98	0.042 57
a	Be [^{1}S]		14.573 02	14.665 99	0.092 98
b	Be [^{1}S][a]		14.573 02	14.616 74	0.043 72
c	Be^{2+} [^{1}S]		13.611 30	13.654 63	0.043 33
d	Be [^{3}P]		14.511 33	14.565 77	0.054 44
e	Be [^{3}P][a]		14.511 33	14.518 42	0.007 09
f	BeH [$^2\Sigma^+$]	2.538	15.153 17	15.245 22	0.091 97
g	BeH [$^2\Sigma^+$]	40.00	15.073 02	15.165 99	0.092 98
h	BeH [$^2\Sigma^+$][a]	2.538	15.153 17	15.198 31	0.045 14
i	BeH [$^2\Sigma^+$][a]	40.00	15.073 02	15.119 03	0.046 02
J	BeH^{3+} [$^1\Sigma^+$]	2.538	12.823 94	12.867 28	0.043 34
k	BeH^{3+} [$^1\Sigma^+$]	40.00	13.561 30	13.604 63	0.043 33

[a] Inner shell electrons not correlated.

one would obtain with full CI computations. Note that careful atomic tabulation[54] reports a correlation energy of −0.043 50 hartrees for Li^{+1}[^{1}S]. From Table 3 we conclude that (1) the inner shell correlation energy is essentially a constant for the ground states of Li^+ [^{1}S] and LiH^{2+} [$X^1\Sigma^+$] at different internuclear separations, (2) our Li^+ [^{1}S] result compared to ref 54 is in error by −0.000 92 hartrees, hereafter denoted "basis set deficiency error", BSDE, and (3) −0.043 50 hartrees is assumed to be the exact value for the $1s^2$ correlation in LiH [$^1\Sigma^+$]. Note that this value does not include the interpair correlation energy $\epsilon(1\sigma-2\sigma)$; from Tables 1 and 3 we obtain $\epsilon(1\sigma-2\sigma) = -0.002\ 22$ hartrees at equilibrium and −0.001 79 at dissociation, the latter to be compared with −0.001 83 hartrees from ref 54. Finally, from Tables 1 and 3, we obtain for LiH [$X^1\Sigma^+$] at dissociation a BSDE of −0.000 97 hartrees. Note that the BSDE relates to total energies, whereas the basis set superposition error, BSSE, refers mainly to binding energies.

An attempt to improve the basis set by decontracting the s and p functions of our basis set and by adding four new 4f and two 5g Gaussian functions with optimized orbital exponents yields a ground-state binding energy of 57.68 kcal/mol, a total energy at equilibrium of −8.069 50 and −7.977 67 hartrees at dissociation; the BSDE is reduced to −0.000 49 hartrees. Handy et al.[63] reported −8.069 04 hartrees at equilibrium and a binding of 57.45 kcal/mol, Cencek and Rychlewski[64] reported a total energy of −8.069 221 hartrees at equilibrium. Recall that after rather easy initial energy gains the total energy improvement from MC expansions becomes a progressively hard computational task.

Concerning the [$A^1\Sigma^+$] excited state we have computed the potential energy curve, see Figure 2, directly at the post-HF−HL accuracy level. This computation is an example of post-HF−HL for an excited state. The computed binding and total energies are 24.10 kcal/mol and −7.945 74 hartrees, respectively, to be compared with the a "recommended value" by Stwalley and Zemke[65] of 24.82 kcal/mol. The computed atomic Li [^{2}S] to Li [^{2}P] excitation energy is 0.067 97 hartrees to be compared with the experimental value of 0.067 91 hartrees.[66] The potential energy has a very flat minimum; with a computed minimum at 5.00 bohr, to be compared with the "recommended value"[65] of 4.91 bohr.

The above computations on LiH demonstrate that reasonable zero-order energies can be obtained with the HF−HL approximation and that very accurate nonrelativistic energies can be determined with the post-HF−HL method.

7. BeH [$X^2\Sigma^+$] Ground State

The literature on the BeH ground state is extensive; we refer to only a few papers.[15,67−73]

In the HF model the BeH [$X^2\Sigma^+$] binding energy is larger than the experimental, a rather rare event in molecular computations, even if not too surprising since the variational principle holds for the total energy of the system and not for arbitrary partitioning.

In the HL theory[3], the BeH [$X^2\Sigma^+$] ground state results from an avoided crossing[68] between the two lowest $^2\Sigma^+$ states analyzed below and more extensively in section 8. The ground state of this molecule is most interesting since to form a bond we need 2p atomic orbitals which are not present in the dissociation products Be [^{1}S]($1s^2 2s^2$) and H [^{2}S]($1s^1$), nor in the HF nor in the HL approximations, unless we consider (a) atomic near-degeneracy, Be [^{1}S]($1s^2 2s^2$) with Be [^{1}S]($1s^2 2p^2$), (b) the inclusion of molecular 2p polarization functions, and (c) avoided curve crossing with the nearest $^2\Sigma^+$ excited state with 2p orbitals.

Near equilibrium the HF(1) function (see inset a of Figure 3) makes use of the 2p basis functions on the Be atom in the 2σ and 3σ molecular orbitals. The 2σ electron population is 0.47 for $2s_{Be}$, 0.28 for $2p_{Be}$, and 1.21 for $1s_H$; the 3σ population is 0.77 for $2s_{Be}$ and 0.33 for $2p_{Be}$. Namely, there is 2s + 2p and 2s − 2p hybridization with bond formation for 2σ and nonbonding single occupation for 3σ. Around the internuclear separation of 4.2 bohr (near the crossing of the two $^2\Sigma^+$ states[3,68]) the HF(1) solution becomes unstable with a clear discontinuity. The binding orbital 2σ becomes a 2s orbital on Be losing the 2p population and the nonbonding 3σ becomes the 1s on the H atom loosing the 2s and 2p population on Be.

With respect to the discontinuity, Mulliken's HF computations[68] reported a slight peak at 4.28 bohr. We recall a detailed discussion by Bagus et al.[70] on the abrupt changes in the electronic structure at internuclear distances between 4 and 6 bohr. Mulliken's maximum in the HF approximation disappears in CI computations.[69−72] From Figure 3a (curve designated HF-(1)) we see clearly the strong binding and the discontinuity in the region around 4.2 bohr (in the figure a vertical line indicates the discontinuity point). With our basis set we obtain HF

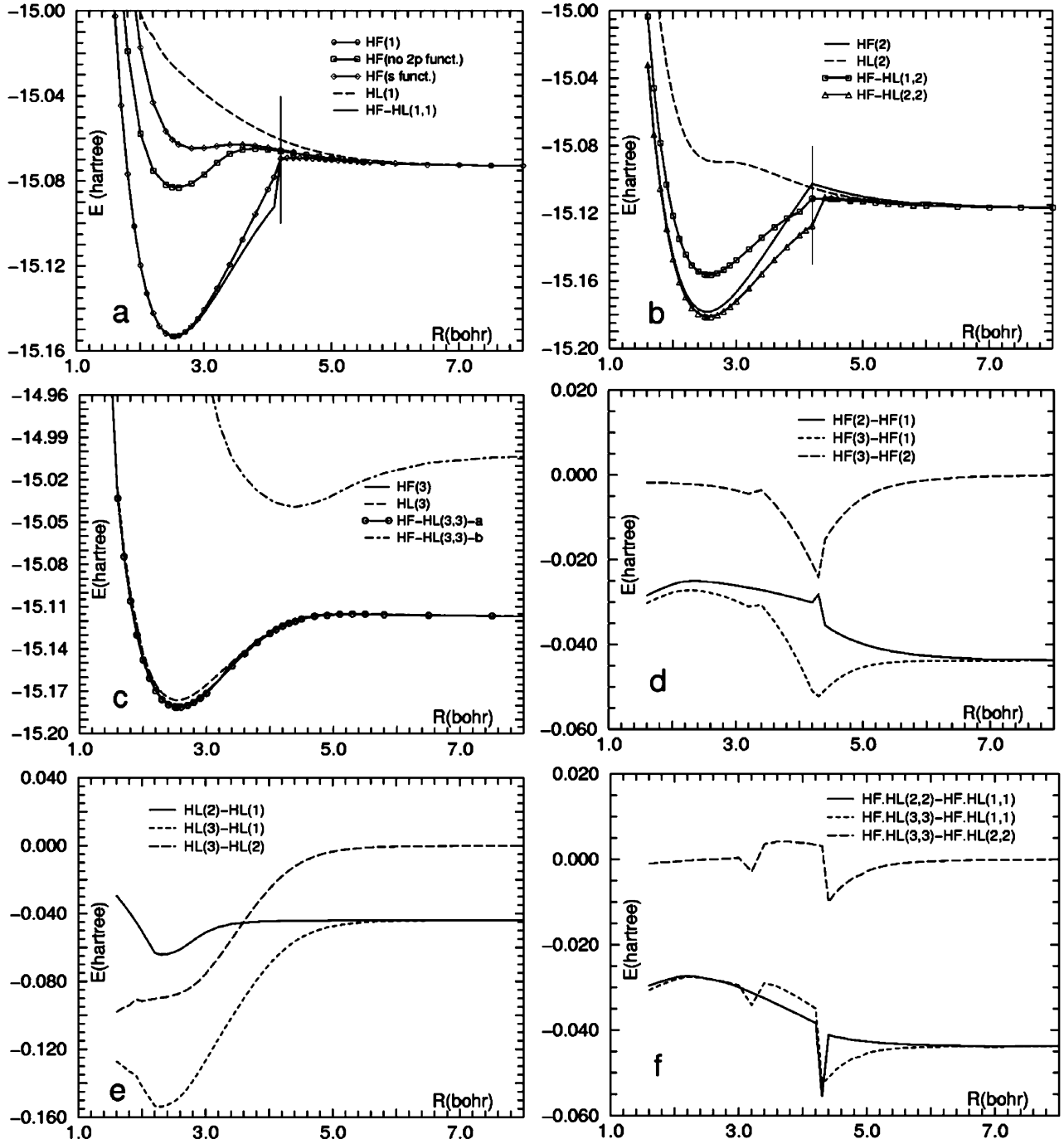

Figure 3. BeH [$^2\Sigma^+$] ground-state potential energy curves: (a) HF, HL, and HF−HL(1,1); (b) HF(2), HL(2), HF−HL(1,2), and HF−HL(2,2); (c) HF(3), HL(3), and HF−HL(3,3); (d) nondynamical and dynamical HF correlation energy contributions; (e) nondynamical and dynamical HL correlation energy contributions; (f) nondynamical and dynamical HF−HL correlation energy contributions.

energies in close agreement with those of ref 70. From our computation we conclude that the HF model is characterized by a discontinuity between 4.20 and 4.28 bohr and a barrier of ~2.40 kcal/mol, not far from Mulliken's barrier of 2.3 kcal/mol. The HF(1) binding energy $E_{b(HF)}$ amounts to 50.29 kcal/mol, obtained as usual by subtracting the sum of the atomic ground-state HF energies of Be [^{1}S] and H [^{2}S] from the molecular HF energy at equilibrium, but neglecting the discontinuity implications (for more details, see the extensive discussion given in the next section).

The presence of the 2p functions in the basis set is essential in order to yield the reported HF binding. To clarify this point, we have performed two new sets of HF computations, one with the basis set detailed in section 1 but deleting the 2p functions (Figure 3a, curve designated "HF(no 2p funct.)"), the second containing only s type functions (i.e., no 2p, no 3d, and no 4f, Figure 3a, curve "HF(s funct.)"). The first computation yields a very weak molecular binding, 6.4 kcal/mol; the second yields no binding, but a marginal repulsion of 5.2 kcal/mol.

To recover the near-degeneracy correlation, a two-configuration MC wave function, labeled HF(2), is obtained from HF-1 and HF-2 (see Table 2). The corresponding curve is given in Figure 3b; it dissociates properly (see Table 4) into the energy sum of the Be [^{1}S] with inclusion of near-degeneracy correlation and H [^{2}S], but we see once more the discontinuity at 4.2 bohr. The binding energy of HF(2) is 38.17 kcal/mol, which is obtained by explicitly including near-degeneracy both at dissociation and at equilibrium. The near-degeneracy stabilization

TABLE 4: Binding Energies (kcal/mol), Total Energies (hartrees), and Correlation Energies (hartrees) from the First Step HF−HL Approximation

computation	BeH [$^1\Sigma^+$]	computation	BH [$^2\Sigma^+$]	CH [$^2\Pi$]
		(a) Without Near-Degeneracy		
$E_{b(HF-HL)}(1,1)$	50.35 (40.43)[a]	$E_{b(HF-HL)}(1,1)$	72.69	67.02
$E_{b(HF)}(1)$	50.29 (40.23)[a]	$E_{b(HF)}(1)$	64.35	57.14
$E_{b(HL)}(1)$	−29.25	$E_{b(HL)}(1)$	72.16	65.82
$E_{(HF-HL)}(1,1)$	−15.153251	$E_{(HF-HL)}(1,1)$	−25.144948	−38.295442
$E_{(HF)}(1)$	−15.153165	$E_{(HF)}(1)$	−25.131587	−38.279666
$E_{(HL)}(1)$	−15.026465	$E_{(HL)}(1)$	−25.144110	−38.293515
$E_{(HF-HL)}(1,1)(R_\infty)$	−15.073009	$E_{(HF-HL)}(1,1)(R_\infty)$	−25.029109	−38.188632
$E_{c(HF-HL)}(1,1)$	−0.093518	$E_{c(HF-HL)}(1,1)$	−0.143002	−0.183250
$E_{c(HF)}(1)$	−0.093607	$E_{c(HF)}(1)$	−0.156363	−0.199026
$E_{c(HL)}(1)$	−0.220307	$E_{c(HL)}(1)$	−0.143840	−0.185177
		(b) With Near-Degeneracy in the HL Component		
$E_{b(HF-HL)}(1,2)$	24.93	$E_{b(HF-HL)}(1,3)$	76.08	67.33
$E_{b(HL)}(2)$	−17.65	$E_{b(HL)}(3)$	75.54	65.93
$E_{(HF-HL)}(1,2)$	−15.156455	$E_{(HF-HL)}(1,3)$	−25.185088	−38.313400
$E_{(HL)}(2)$	−15.088603	$E_{(HL)}(3)$	−25.184222	−38.311167
$E_{(HF-HL)}(1,2)(R_\infty)$	−15.116733	$E_{(HF-HL)}(1,3)(R_\infty)$	−25.063842	−38.206103
$E_{c(HF-HL)}(1,2)$	−0.003204	$E_{c(HF-HL)}(1,3)$	−0.102862	−0.165292
$E_{c(HL)}(2)$	−0.158169	$E_{c(HL)}(3)$	−0.103728	−0.167525
		(c) With Near-Degeneracy in the HF Component		
$E_{b(HF-HL)}(2,1)$	38.79	$E_{b(HF-HL)}(4,1)$	77.08	69.91
$E_{b(HF)}(2)$	38.65	$E_{b(HF)}(4)$	77.08	69.73
$E_{(HF-HL)}(2,1)$	−15.178555	$E_{(HF-HL)}(4,1)$	−25.187442	−38.317605
$E_{(HF)}(2)$	−15.178325	$E_{(HF)}(4)$	−25.186678	−38.317225
$E_{(HF-HL)}(2,1)(R_\infty)$	−15.116733	$E_{(HF-HL)}(4,1)(R_\infty)$	−25.063842	−38.206194
$E_{c(HF-HL)}(2,1)$	−0.068217	$E_{c(HF-HL)}(4,1)$	−0.100508	−0.161085
$E_{c(HF)}(2)$	−0.068447	$E_{c(HF)}(4)$	−0.101272	−0.161465
		(d) With Near-Degeneracy in the HF and HL Components		
$E_{b(HF-HL)}(2,2)$	40.50	$E_{b(HF-HL)}(4,3)$	77.78	70.03
$E_{(HF-HL)}(2,2)$	−15.181269	$E_{(HF-HL)}(4,3)$	−25.187796	−38.317713
$E_{(HF-HL)}(2,2)(R_\infty)$	−15.116733	$E_{(HF-HL)}(4,3)(R_\infty)$	−25.063842	−38.206109
$E_{c(H-HLF)}(2,2)$	−0.065503	$E_{c(H-HLF)}(4,3)$	−0.100154	−0.160979

[a] Rationalized HF and HF−HL binding energies from HF(3) and HF−HL(3,3).

at dissociation is −0.042 72 hartrees (exactly equal to the value for the Be [^{1}S] atomic near-degeneracy) but only −0.025 16 hartrees at equilibrium (notably smaller than at dissociation, at equilibrium "the Be atom in the molecule" is "less near-degenerate" relative to Be at dissociation since with larger energy difference).

In Figure 3c, we present a three MC configuration computation, labeled HF(3), where we have extended the previous two MC configurations by including HF-3 (see Table 2); the latter contains a 4σ molecular orbital belonging to the first excited BeH [$C^2\Sigma^+$] state, which dissociates into Be [^{3}P] and H [^{1}S]. The motivation for this computation is to verify that the discontinuity and the energy barrier originate from state crossing. Indeed, the inclusion of this configuration leads to the HF(3) computation with the elimination of the discontinuity and a decrease on the barrier height. The binding of HF(3) is 40.23 kcal/mol, and the energy at dissociation is −15.116 73 hartrees (as for HF(2), see Table 4).

We now consider the HL approximation. We note that BeH $[X^2\Sigma^+](1s^22s^2)_{Be}(1s^1)_H$ has an electron pair 2s localized on Be and a single electron on H. The near-degenerate state BeH $[C^2\Sigma^+](1s^22p^2)_{Be}(1s^1)_H$ has a pair 2p on Be but again a single electron on H; in both situations there is no electron on Be free to form a bond with the $(1s^1)_H$. Therefore, we expect a repulsion in the HL approximation from the configuration Be $(^1S)(1s^2\text{-}2s^2)_{Be}$ either with or without addition of the Be $(^1S)(1s^22p^2)_{Be}$ near-degenerate configuration. Indeed, the HL computations yield no binding, and we obtain a repulsion of about 29 kcal/mol at the laboratory equilibrium internuclear distance (see Figure 3a, curve labeled HL(1)). Also inclusion of the near-degenerate state Be $[^1S](1s^22p^2)_{Be}$ in two MC−HL configurations $(1s^1)_H(1s^22s^2)_{Be}$ and $(1s^1)_H(1s^22p^2)_{Be}$ yields no bond formation, but the repulsion is reduced to about 16 kcal/mol (see Figure 3b, curve labeled HL(2)). In the latter case the nondynamical correlation penetrates from very large to shorter internuclear separations, and at near equilibrium position it produces an inflection point (see Figure 3b**)**. Inclusion of the third configuration leads to HL(3) (see Figure 3c), which is bound by 37.37 kcal/mol. We shall discuss in detail the avoided crossing in the next section.

In the HF−HL approximation we have performed three computations reported in Figure 3: HF−HL(1,1) given in panel a, HF−HL(1,2) and HF−HL(2,2) given in panel b, and HF−HL(3,3) given in panel c. From Figure 3 it is evident that the HF−HL energies are lower than the corresponding HF or HL energies. Panel a shows that the HF−HL(1,1) potential curve suffers from the Hartree−Fock discontinuity problem; the binding energy is 50.35 kcal/mol. The function HF−HL(1,2) yields a binding energy of 24.93 kcal/mol, and again it shows the discontinuity. In addition it presents a rather anomalous behavior in the region of 3.4−4.0 bohr (see panel b). We attribute this anomalous behavior to the lack of balance between HF and HL components; inclusion of nondynamical correlation in only the HL (or in only the HF function) brings about an "unbalanced" situation. The HF−HL(2,2) balanced computation (see Figure 3b) appears more reliable; it provides a reasonable computed binding, 39.99 kcal/mol and has no anomalous behavior in the region of 3.4−4.0 bohr, but it does show the discontinuity.

Inclusion of the third configuration leads to HF(3), HL(3) discussed above and to a two-root solutions HF−HL(3,3)-a and HF−HL(3,3)-b (Figure 3c) generating avoided crossing. The

lower root HF−HL(3,3)-a eliminates the discontinuity and brings about a binding of 42.71 kcal/mol to be compared with 40.23 kcal/mol for HF(3) and 37.37 for HL(3). The molecular extracorrelation energy is 7.12 kcal/mol and the barrier height is 0.92 kcal/mol. The upper root HF−HL(3,3)-b dissociates into Be [^{3}P]($1s^2 2s^1 2p^1$) and H [^{2}S] ($1s^1$) and its minimum energy is shifted to about 4.2 bohr, which is the crossing point.

In Figure 3d−f we analyze in detail the contributions related to the nondynamical correlation energy for the HF (panel d), HL (panel e), and for the HF−HL functions (panel f). In panel d, the energy differences [HF(2)−HF(1)] is the nondynamical HF correlation energy, which is approximately constant until the discontinuity and thereafter increases to 0.043 72 hartrees, the same value we have computed for the near-degeneracy correlation in Be [^{1}S]. The difference [HF(3)−HF(1)] represents the sum of the nondynamical correlation discussed above and of the correlation gained by including avoided crossing. This correlation correction pattern follows the previous one but has a marked increase in the region of the discontinuity, confirming that avoided crossing is needed to eliminate the discontinuity. In the figure the avoided crossing energy stabilization is designated HF(3)−HF(2).

The nondynamical correlation associated with the HL functions is considered in Figure 3e. The main result is that the HL nondynamical correlation is notably larger than the corresponding HF quantities. Note the large contribution at short internuclear separations. At equilibrium the near-degeneracy stabilization is 0.062 14 hartrees, notably higher than for HF.

Finally in Figure 3f, we report the cumulative HF and HL correlation correction gains obtained from the HF−HL approximation. The HF−HL data resemble more those for HF than those for HL, since the correlation diagrams do not add up the separated effects (panels d and e) due to the different weights of the HF and HL components in the HF−HL function at different internuclear separations.

A summary of the computed total energies at the equilibrium distance and at dissociation, the corresponding correlation energy contributions, and the binding energies are given in Table 4.

8. BeH: Binding Energy of the [$X^2\Sigma^+$] State and Avoided Crossing with [$C^2\Sigma^+$]

We consider in detail the avoided state crossing of the [$X^2\Sigma^+$] ground state with the first excited state [$C^2\Sigma^+$] using the HL approximation, which allows us to follow very nicely this process. On the contrary, note the difficulties in following the crossing within the HF approximation.[73] In Figure 4 we report the previous HL computations for HL(1) and HL(2) and a new computation for HL-3 (see Figure 4), which dissociates into Be [^{3}P]($1s^2 2s^1 2p^1$) and H [^{2}S]($1s^1$). We have computed the avoided crossing by making the linear combination of HL(1) and HL-3, yielding a lower and an upper solution (curves labeled a and a′) with binding energies of 41.39 and 9.26 kcal/mol at an internuclear separation of 2.8 and 5.0 bohr, respectively. Further, we have considered the linear combination of HL(2) and HL-3, thus including the effect of near-degeneracy (solutions designated b and b′). For HL-b and HL-b′ the minimum is shifted to ∼2.6 and 4.4 bohr, the binding energies are 31.41 and 17.81 kcal/mol, respectively.

The determination of the ground-state binding energy requires a post-HF−HL computation. First, we verify the capability of our basis set to yield accurate binding and total energies, adopting a well-established MC approach, the CASSCF. We expect to obtain energies at the same accuracy level one would obtain by performing the somewhat more laborious computations required for the three MC expansions of the second and third HF−HL steps (eqs 5 and 6).

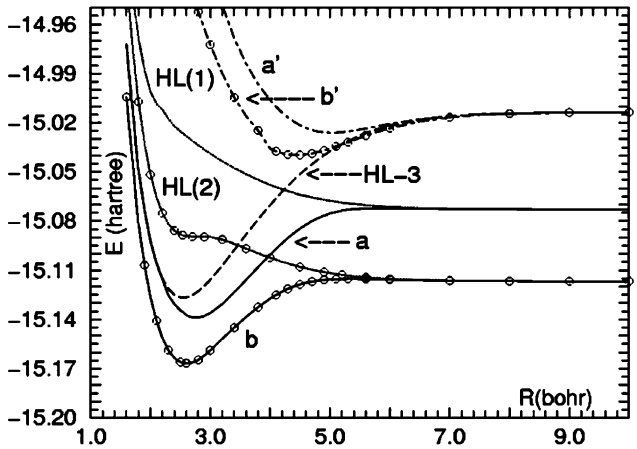

Figure 4. BeH [$^2\Sigma^+$]: HL potential energy for HL(1), HL(2), HL-3, and avoided state crossings. Curves a and a′ are obtained by variationally combining HL(1) and HL-3; those indicated with b and b′, by variationally combining HL(2) and HL-3.

In Table 3 we report HF, CASSCF, and correlation energy data all obtained with the same basis set (section 1) at 2.583 bohr (equilibrium distance) and at 40 bohr (full dissociation). The CASSCF computations have been carried out with all the available orbitals in the active space, except for cases f and g, where 80 active orbitals hae been considered. The computed molecular dissociation energy values are confirmed by atomic computations. Further, to analyze the correlation energy data, we include computations with frozen core (either $1s^2$ or $1\sigma^2$) and those for the ions Be^{2+} [^{1}S] and BeH^{3+} [$^1\Sigma^+$]. To each computation we assign an alphabetical index from "a" to "k".

Concerning the binding energy the computed value (from f and g in the table) yields 49.72 kcal/mol very close to the experimental value of 49.83 kcal/mol. The frozen core computations h and i yield a binding of 49.75 kcal/mol. The computed excitation energy Be [^{1}S] to Be [^{3}P] is 2.727 eV (from a and d) to be compared to 2.725 eV from laboratory data[66] and to 2.675 eV by using frozen core energies (b and e).

The computed total energy at equilibrium is −15.245 23 hartrees, to be compared to −15.2457(2) and −15.2231(8) hartrees, from diffusion quantum Monte Carlo and variational quantum Monte Carlo computations,[61] respectively. To our knowledge, this is the most accurate computation in the literature for the BeH [$X^2\Sigma^+$] binding and total energies from ab initio variational methods. Among the many previous computations we recall bindings of 48.77 [70] and 48.88 kcal/mol,[71] and the corresponding total energies of −15.196 35 and −15.196 76 hartrees, both obtained with the frozen core approximation.

The computed correlation energies for Be [^{1}S] and for BeH [$X^2\Sigma^+$] are −0.092 98 and −0.092 06 hartrees, respectively (see a and f). From the data in Table 3 we can decompose the Be correlation energy into the pairs $\epsilon(1s^2)$ and $\epsilon(2s^2)$ and the interpair $\epsilon(1s-2s)$. For BeH the pairs are $\epsilon(1\sigma^2)$ and $\epsilon(2\sigma^2)$ and the interpairs $\epsilon(1\sigma-2\sigma)$, $\epsilon(1\sigma-3\sigma)$, and $\epsilon(2\sigma-3\sigma)$. For Be [^{1}S] we obtain $\epsilon(1s^2) = -0.043\,33$ hartrees (from entry c in Table 3), $\epsilon(2s^2) = -0.043\,72$ hartrees (from b), and $\epsilon(1s-2s) = -0.005\,93$ hartrees (subtracting b and c from a). For BeH [$X^2\Sigma^+$] we obtain $\epsilon(1s^2) = -0.043\,34$ hartrees (from j), $[\epsilon(2\sigma^2) + \epsilon(2\sigma-3\sigma)] = -0.045\,14$ hartrees (from h), $[\epsilon(1\sigma-2\sigma) + \epsilon(1\sigma-3\sigma)] = -0.002\,70$ hartrees (subtracting i and j from f). Note that $\epsilon(1s^2)$ and $\epsilon(1\sigma^2)$ are essentially equal, as found for LiH. The correlation energy difference, $\Delta\epsilon$, for Be [^{1}S] and BeH

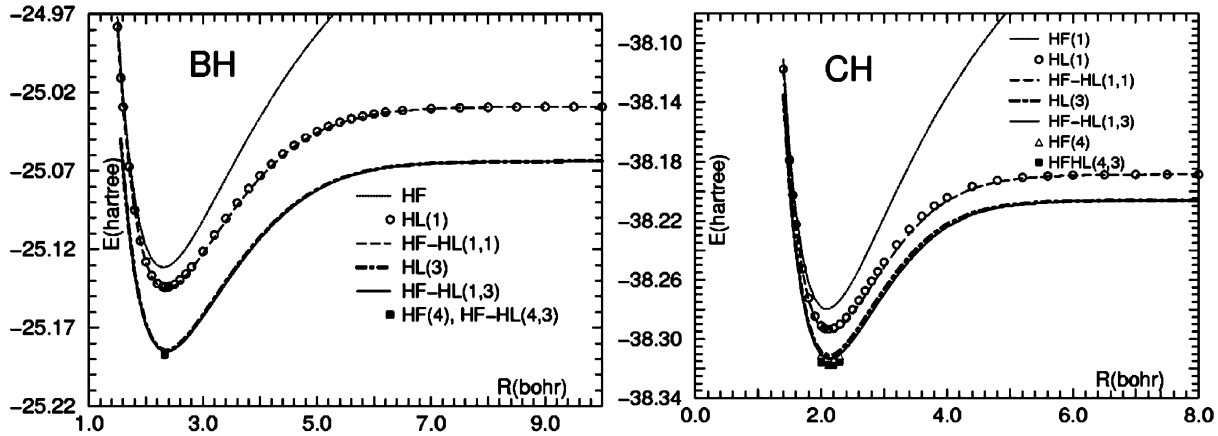

Figure 5. BH [$^1\Sigma^+$] (left panel) and CH [$^2\Pi$] (right panel) potential energy curves for HF, HL, and HF−HL approximations with and without nondynamical correlation, unbalanced or balanced.

[$X^2\Sigma^+$], namely, the molecular extra correlation energy, amount to 0.0009 hartrees (analyzed later).

Thus, we have verified that our basis set is adequate to yield accurate binding energy determinations and very reasonable for nonrelativistic total energy computations.

In the previous section we have reported an HF binding energy of 50.29 kcal/mol obtained as usually done by subtracting the sum of the atomic ground-state HF energies for Be [^{1}S] and H [^{2}S] from the molecular HF computed energy at equilibrium. The above binding energy value appears rather anomalous since (1) it is obtained assuming a regular molecular HF function, rather than the one with a discontinuity (resulting from state crossing) and likely contaminated by near-degeneracy, (2) it is very close (indeed larger) to the laboratory value of 49.83 kcal/mol, and (3) the molecular extracorrelation energy is exceptionally a positive, even if small, value, 0.58 kcal/mol.

We can follow two paths to explain the rather surprisingly binding energy value. The first simply states that the correlation energy of the five electrons in BeH at the equilibrium geometry is nearly equal to the correlation energy of the four electron atom Be [^{1}S]. This appears to be in contrast with the generally accepted rule according to which the correlation energy increases with the number of electrons. However, exceptions to the above rule have been recently reported in atomic systems[74] with near-degeneracy effects, similarly to the BeH case.

The second paths considers an artifact the HF correlation energy obtained following the traditional definition, in the case of BeH, since the HF(1) solution exhibits a singularity at the curve crossing. This alternative path stresses the existence of the HF discontinuity with two and not one HF solution, and the consequent need to account for the avoided crossing before computing the correlation energy. We recall that, since long ago,[9] it was proposed that a single determinant is only one among several formulations of the general HF model: in particular situations (such as for near-degeneracy in atomic systems) short MC functions are the HF-type functions of preference. Curve crossing is another particular situation of high relevance in molecular systems. The HF(3) function appears to be a reasonable replacement for the HF(1) function for the correlation energy computation of BeH. Its binding energy of 40.23 kcal/mol eliminates the problem related to a positive value of the extracorrelation energy. The correlation and molecular extracorrelation energy are thus −0.065 49 and −0.014 66 hartrees, respectively. Note that this value is indirectly supported by the computed binding energies 37.37, 41.39, and 42.71 kcal/mol from HL(3), from the combination of HL-3 with HL-1 and from HF−HL(3,3), respectively. In section 11 the rationalized binding energy is once more suggested by comparing data for the full set of monohydrides. The value of 40.23 kcal/mol is therefore reported in Table 4 in correspondence of the HF binding energy.

Note that these computations bring us once more to the conclusion that the physically meaningful reference function for BeH can be neither the Hartree−Fock function, which is plagued by instabilities and ambiguities, nor the Heitler−London, which is incapable of yielding molecular binding.

9. BH [$^1\Sigma^+$] and CH [$^2\Pi$]

The BH [$^1\Sigma^+$] and the CH [$^2\Pi$] analysis is relatively simpler than that for BeH [$^2\Sigma^+$] since there is 2p atomic orbital availability for bond formation both in B [^{2}P]($1s^2 2s^2 2p^1$) and in C [^{3}P]($1s^2 2s^2 2p^2$) and since the near-degeneracy in the B and C atoms is relatively weaker than in the Be one. However, the BH [$^1\Sigma^+$] and the CH [$^2\Pi$] computations of the near-degeneracy require two added configurations, the $1s^2 2s^0 2p^3$ and $1s^2 2s^1 2p^2$ for the B atom and the $1s^2 2s^0 2p^4$ and $1s^2 2s^1 2p^3$ for the C atom.

In Figure 5, we report the HF, HL, and HF−HL potential energy curves for BH [$^1\Sigma^+$] (left inset) and for CH [$^2\Pi$] (right inset). The computed HF, HL, and HF−HL bindings for BH [$^1\Sigma^+$] are 64.36, 72.16, and 76.08 kcal/mol. respectively, at the internuclear separation of 2.329 bohr. In computing the HF near-degeneracy, we include a forth function, HF-4 (see Table 2), needed to yield a correct dissociation. The BH [$^1\Sigma^+$] correlation energies in the HF(4), HL(3), and HF−HL(4,3) functions are −0.101 27, −0.103 73, and −0.100 15 hartrees, respectively, and the binding energies are 77.08, 75.54, and 77.78 kcal/mol, respectively.

The HF−HL(1,3) combination of the HF(1) function and HL-(3) functions yields a binding of 76.08 kcal/mol; note however that this is an unbalanced computation. A balanced computation HF−HL(4,3) yields a binding energy of 77.78 kcal/mol. This computation has been performed for three points in the neighborhood of the equilibrium internuclear separation and differs only slightly from HF−HL(1,3).

The CH [$^2\Pi$] potentials, reported in Figure 5, are computed with and without inclusion of nondynamical correlation. These computations follow the same pattern as those for the BH molecule. The computed HF, HL, and HF−HL bindings for CH [$^2\Pi$] are 57.14, 65.82, and 67.82 kcal/mol, respectively, at the internuclear separation of 2.122 bohr. The CH[$^2\Pi$] dynamical correlations energies in the HF(4), HL(3), and HF−HL-(4,3) functions are −0.161 48, −0.167 53, and −0.160 97 hartrees, respectively, and the binding energies are 69.73, 65.93, and 70.03 kcal/mol, respectively.

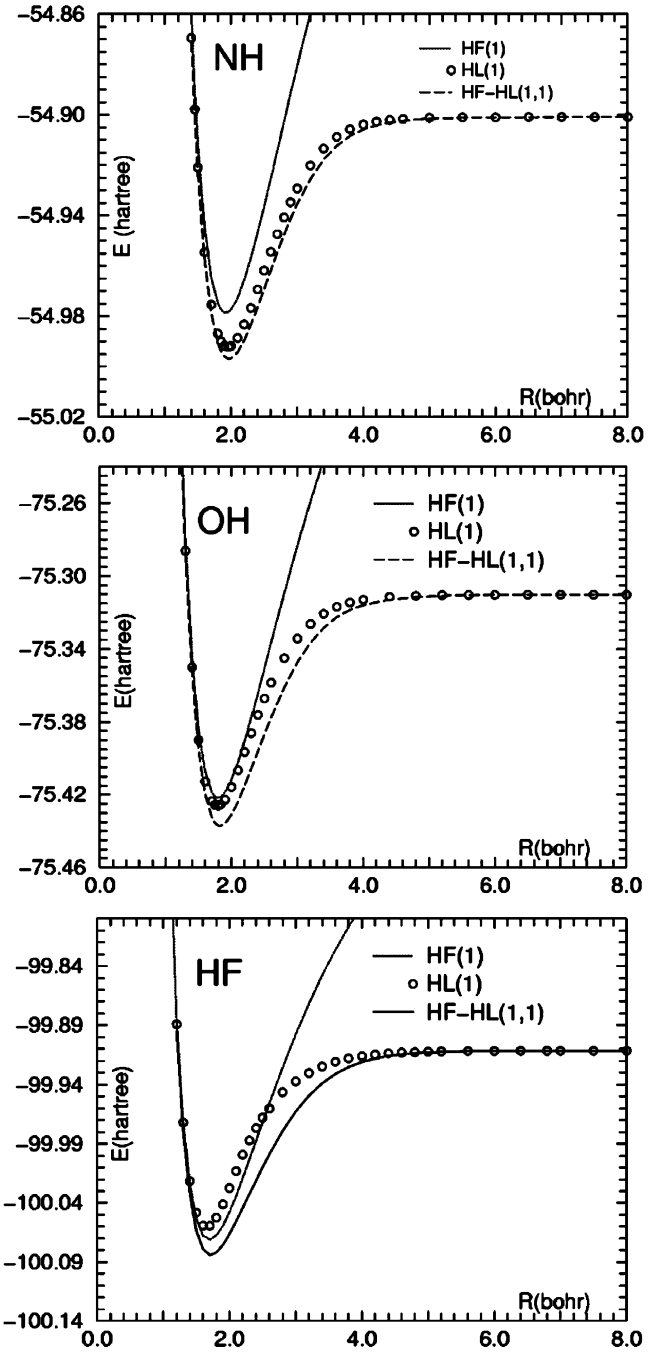

Figure 6. HF, HL, and HF−HL potentials for NH [$^3\Sigma^-$] (top panel), OH [$^2\Pi$] (middle panel), and HF [$^1\Sigma^+$] (bottom panel).

A detailed analyses of the computed energies shows a nearly constant nondynamical correlation energy for any internuclear distance. The variation of the weights for the HF and HL components show a dominant HL presence from short distances to dissociation.

In Table 4 for BeH [$X^2\Sigma^+$], BH [$^1\Sigma^+$], and CH [$^2\Pi$], we summarize the HF(n), HL(m), and HF−HL(n,m) computational data at dissociation and at the experimental equilibrium distance (the latter given in Table 1). For each molecule, we report the binding energies (in kcal/mol), $E_{b(HF-HL)}$, $E_{b(HF)}$, and $E_{b(HL)}$; the total energies (in hartrees), $E_{(HF-HL)}$, $E_{(HF)}$, $E_{(HL)}$, and $E_{(HF-HL)}(R_\infty)$ at dissociation; and the correlation energies, $E_{c(HF-HL)}$, $E_{c(HF)}$, and $E_{c(HL)}$. We tabulate the following separately: (a) the energies without near-degeneracy, (b) near-degeneracy in the HL component (indices 1,2 for BeH, 1,3 for BH and CH), (c) inclusion of near-degeneracy in the HF component (indices 2,1 for BeH, 4,1 for BH and CH), and (d) inclusion of near-degeneracy in the HF and HL components (indices 2,2 for BeH, 4,3 for BH and CH).

TABLE 5: Binding Energy, $E_{b(HF-HL)}(1,1)$ (kcal/mol), Total Energy (hartrees) at Equilibrium, $E_{(HF-HL)}(1,1)(R_e)$, and at Dissociation, $E_{(HF-HL)}(1,1)(R_\infty)$, and Correlation Energy $E_{c(HF-HL)}(1,1)(R_e)$ from the First Step HF−HL Approximation

computation	H_2 [$^1\Sigma^+$]	LiH [$^1\Sigma^+$]	NH[$^2\Pi$]	OH [$^3\Sigma^-$]	HF [$^1\Sigma^+$]
$E_{b(HF-HL)}$	94.50	43.66	60.29	79.62	108.36
$E_{b(HF)}$	83.83	34.27	48.59	70.16	101.23
$E_{b(HL)}$	94.28	43.11	57.30	72.26	92.17
$-E_{(HF-HL)}$	1.150595	8.002298	54.997006	75.437153	100.084049
$-E_{(HF)}$	1.133599	7.987338	54.978355	75.421187	100.070665
$-E_{(HL)}$	1.150247	8.001415	54.992242	75.425426	100.058248
$-E_{(HF-HL)}(R_\infty)$	0.999999	7.932719	54.900922	75	99.911365
$-E_{c(HF-HL)}$	0.023873	0.068193	0.220534	0.299927	0.375151
$-E_{c(HF)}$	0.040872	0.083153	0.239185	0.315893	0.388535
$-E_{c(HL)}$	0.024221	0.069076	0.225298	0.311654	0.400952

The tabulation of the four cases has been reduced in length by reporting specific energy data only for the first presence in the table; for example the HF(1) energy is relevant in the a and b subtabulations but is given only in a.

10. HF−HL Model for NH [$^3\Sigma^-$], OH [$^2\Pi$], and HF [$^1\Sigma^+$]

For the ground-state molecules NH [$^3\Sigma^-$], OH [$^2\Pi$], and HF [$^1\Sigma^+$], the HF−HL computations are equivalent to those for LiH, since there is no near-degeneracy in the N [^{4}S], O [^{3}P], and F [^{2}P] atoms. Therefore, for these molecules the only contribution to the nondynamical correlation energy is that gained by mixing HF and HL functions. The computed HF, HL, and HF−HL potential energy curves are reported in Figure 6. In Table 5 we report, for the experimental equilibrium distance, the binding energies (in kcal/mol), $E_{b(HF-HL)}$, $E_{b(HF)}$, and $E_{b(HL)}$; the total energies (in hartrees), $E_{(HF-HL)}$, $E_{(HF)}$, $E_{(HL)}$, and $E_{(HF-HL)}(R_\infty)$ at dissociation; and the correlation energies, $E_{c(HF-HL)}$, $E_{c(HF)}$, and $E_{c(HL)}$. In Table 5 we also report data for H_2.

For NH [$^3\Sigma^-$], OH [$^2\Pi$], and HF [$^1\Sigma^+$] the HF binding amounting to 48.59, 70.16, and 101.23 kcal/mol, respectively, increases to 60.29, 79.62, and 108.36 kcal/mol, respectively, in the HF−HL approximation. The HL binding is deeper than the HF binding for H_2, LiH, NH, and OH but not for HF.

We conclude that, for all the hydrides considered in this work, the HF−HL approximation is superior to either the HF or the HL approximations.

Furthermore, we recall that, in the present HF−HL first-step approximation, we have not considered ionic structures for the HL component. Inclusion of two of these structures for the HF molecule leads to a HF−HL computation with five configurations (HF, HL covalent, HL ionic F^-H^+, and HL ionic F^+H^-), yielding a binding of 132.5 kcal/mol. A very extensive CASSCF (8,22) computation (8 electrons into an active space of 22 orbitals, generating over 13 million determinants) yields a binding energy of 131.99 kcal/mol. This comparison shows that very compact HF−HL functions can yield not only correct dissociation but also reasonable binding energies.

11. HF, HL, and HF−HL Binding Energies

In Figure 7 we consider two quantities: In the top panel the binding energies from HF, HF−HL, and the experimental data, in the bottom panel the molecular extracorrelation energy from the HF and the HF−HL models. Concerning the binding energy, we recall that the HeH and the NeH have exceedingly small binding energies (not visible on our scale), marking the beginning and the end to the second period hydrides. The

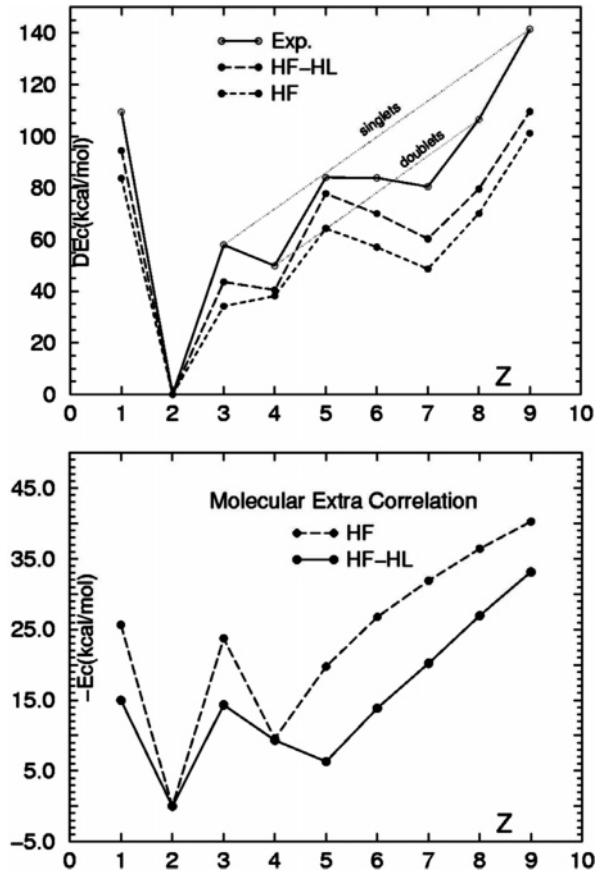

Figure 7. Top: Hydride binding energies from the HF and HF−HL approximations and from experiments. Bottom: Molecular extracorrelation energy from the HF and HF−HL models.

seemingly irregular behavior of the experimental data is a manifestation of an empirical rule for this *sequence* of homogeneous molecules, the monohydrides: *for a given period of the atomic table the hydrides with the same spin multiplicity have binding linearly increasing with the number of electrons, and the higher the spin multiplicity, the higher the binding*. Recall that the ground state for LiH, BH, and HF is a singlet state, for BeH, CH, and OH is a doublet state, and for OH is a triplet state. (A nearly equivalent rule is known from correlation energy studies in atomic sequences[75]). The HF−HL model predicts a binding energy pattern which closely follows the experimental one, with 81% average agreement. For the HF and HL models the computed binding has an average agreement of 69 and 66%. In computing the above average errors, we have not considered the repulsive energies.

In the bottom panel of Figure 7 we display the molecular extracorrelation energy, namely, the error of the HF and HF−HL computed molecular binding. For H_2 and LiH the binding energy errors are approximately equal, 14.5 and 15.3 kcal/mol from HF−HL computations, and 35.6 and 23.73 kcal/mol from HF computations, respectively. For bonds formed with 2p electrons (and this includes also BeH due to the near-degeneracy) both models, HF and HF−HL, present correlation energy patterns that smoothly increase with *Z*.

12. HF and HF−HL Correlation Energies

It is of interest to compare (1) atomic and molecular correlation energies, $E_c(n)$, in systems characterized by n electrons and (2) in the hydrides the values of $E_c(n)$ at the united atom, at equilibrium and at dissociation. The comparison brings

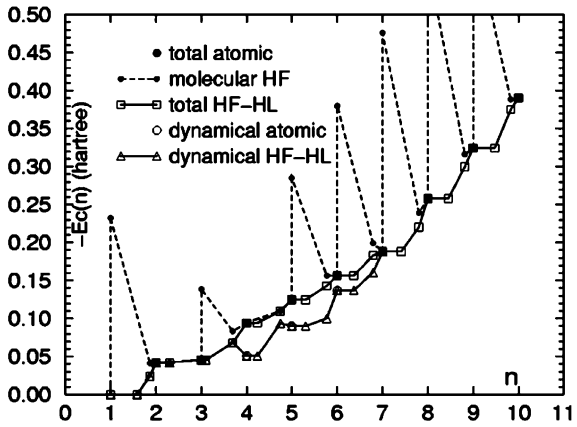

Figure 8. Total and dynamical atomic and molecular correlation energies. See text for details.

in evidence of the shortcoming of the HF model and the relative superiority of the HF−HL model.

In Figure 8, using data from Tables 1, 4, and 5, we report the $E_c(n)$ values in the ordinate versus n in the abscissa, where n represents the number of electrons both in the atomic and in molecular systems. In addition, the abscissa represents the internuclear distances: for a XH(n) hydride, $E_c(n)$ varies from the internuclear separation $R(XH) = 0$ bohr plotted at n on the abscissa, to $R(XH) = 10$ bohr made to correspond to $n - 1$. Alternatively stated, each interval, n to $n - 1$, also represents the scaled internuclear separations from $R(XH) = 0$ to $R(XH) = 10$ bohr, which corresponds essentially to dissociation.

In Figure 8 we plot the total HF atomic correlation energies (full bullet) without and with near-degeneracy. In addition, for the hydrides at a few internuclear separations, we report the correlation energies $E_{c(HF)}$ connected by a dashed line, the total $E_{c(HF-HL)}$ (square marks connected by a solid line), and the dynamical $E_{c(HF-HL)}$ (triangle marks connected by a solid line). The atomic correlation energy value for the atom with $Z = n$ is equal to the correlation energy of XH(n) at the united atom, $R(XH) = 0$, both in the HF−HL and HF approximations. In addition, the atomic correlation energy value for the atom with $Z = n - 1$ corresponds to the correlation energy of XH(n) at dissociation, $R(XH) = \infty$ in the HF−HL approximation, but not for the HF approximation, which breaks down approaching dissociation (exception made for BeH). The HF correlation energy increases sharply concomitant with the HF model breakdown; in the graph we have reported the HF correlation at the united atom, at the equilibrium internuclear distance, and at $R(XH) = 10$ bohr. The HF−HL correlation energy is reported at the united atom, at the equilibrium internuclear distance, at $R(XH) = 3R_e$ and at $R(XH) = 10$ bohr. Note that at $R(XH) = 3R_e$ the HF−HL correlation is essentially equal to its value at dissociation.

From the figure it is evident that the atomic correlation energy is the dominant component of the hydrides total molecular correlation, exception made for those containing very few electrons. Note that the difference in spin multiplicity comparing the XH molecule and the X atom for $n = 6$ (^{3}P and $^1\Sigma$) and $n = 7$ (^{4}S and $^2\Pi$) appears to be rather unimportant, at least for the energy scale of the figure. The role of the molecular extracorrelation in molecular binding is evident, but at the same time the overall graph shows that the XH systems are essentially perturbed atoms, especially for large values of n. Finally, the graph clearly points out that the HF representation becomes physically meaningless shortly after equilibrium (approximately after $R(HX) = 2R_e$) up to dissociation, whereas the HF−HL

TABLE 6: Dipole Moments (*D*) from HF, HL, *Simple* HF−HL, and Experiments

model		LiH	BeH	BH	CH	NH	OH	HF
HF	$\mu(R_e)$	6.00	0.14	1.31	1.31	1.61	1.76	1.92
	$\Delta\mu$	0.25	0.09	0.17	0.20	0.03	0.05	0.10
HL	$\mu(R_e)$	5.72	0.06	1.37	1.37	1.55	1.79	1.75
	$\Delta\mu$	0.18	0.08	0.14	0.15	0.05	0.03	0.02
HF−H L	$\mu(R_e)$	5.83	0.15	1.32	1.33	1.57	1.75	1.85
	$\Delta\mu$	0.21	0.10	0.14	0.17	0.05	0.04	0.07
expt		5.88[a]		1.27 ± 0.21[b]	1.46[c]	1.39[a]	1.67[a]	1.83[a]

[a] Reference 76. [b] Reference 77. [c] Reference 78.

representation is realistic from the united atom to dissociation. The fact that HF−HL is the model of preference at any internuclear distance shows that it is the "reference function" for molecular systems.

For BeH [$X^2\Sigma^+$] we have plotted for $n = 4$ to $n = 5$ the value for the correlation energy which corresponds to the rationalized binding energy of 40.23 kcal/mol.

13. Dipole Moment for the Second Row Hydrides

We have shown that, at a very moderate incremental cost in computational complexity, the HF−HL model notably improves the realism in bond energy prediction, from united atom to dissociation, relative to the HF and HL models. The dipole moment, μ, is another basic observable in modeling the electronic structure of molecules. The dipole moment for the hydrides of the second row, reported in Table 6, is obtained from computations in the HF, HL, and HF−HL models and from experiments.[76−78] The HF−HL method appears reliable also for dipole moment computations. In addition we stress that the computed HF−HL dipole moment in the HF−HL approximation goes correctly to zero at dissociation, whereas the HF model often yields dipole moment values totally unphysical at large internuclear separations.

The reported values of μ are for the equilibrium distance; we recall that μ varies strongly with the internuclear distances, yielding maxima and minima. This observation suggests to report the $|\Delta\mu|$ for two distances R_1 and R_2, with $R_1 < R_e < R_2$ and $\Delta R = R_1 - R_2 = 0.2$ bohr. From the table we see that the computed value of μ, taking into account $|\Delta\mu|$ brackets the experimental value.

14. Conclusions

We have presented a new variational computational method, the Hartree−Fock−Heitler−London and compared Hartree−Fock, Heitler−London, and Hartree−Fock−Heitler−London potential energy curves for the first and second period hydrides. Keeping in mind preliminary computations[29] for Li_2 and F_2, we conclude that neither the HF nor the HL approximation is capable of systematically reproducing, at least qualitatively, the basic molecular binding features known experimentally (bond breaking and bond formation). Further, the HF model breaks down at dissociation, preventing any assessment of the correlation correction for internuclear separations larger than about twice the equilibrium distance. The two traditional methods, however, have the high merits of mathematical simplicity and immediate physical interpretability and, because of these two basic qualities, have historically provided two distinct quantum chemical "reference" wave functions for theoretical and computational chemistry. More importantly, the two methods are at the origin of the most basic concepts in physical chemistry and in chemical physics.

The HF−HL method merges the two historical paths, at a marginal increase in computational complexity, retaining at the same time the physical interpretability of the two original contributions. The combination of the two methods into the HF−HL approach eliminates grossly unphysical aspects, particularly at large internuclear separations, and accounts for nondynamical correlation and state crossing. Furthermore, the HF−HL approach systematically predicts molecular binding more correctly than those obtained from either the Hartree−Fock or the Heitler−London models. Finally, by reducing the correlation energy error to its dynamical component, it simplifies the computational task in post-HF−HL computations.

Therefore, the HF−HL approach provides a reliable "zero-order reference wave function", while maintaining mathematical simplicity and immediate physical interpretability based on the two traditional chemical models, LCAO-MO and VB.

Acknowledgment. It my pleasure to thank Enrico Clementi for suggesting the topic, for help in the manuscript preparation, and for providing some of the computational facilities. A grant from MIUR-2004034838 is acknowledged.

References and Notes

(1) Hund, F. R. *Z. Phys.* **1927**, *40*, 742.
(2) Mulliken, R. S. *Phys. Rev.* **1928**, *32*, 186.
(3) Herzberg, G. *Spectra of Diatomic Molecules*; Van Nostrand: Princeton, N J, 1951; and references cited therein.
(4) Heitler, W.; London, F. *Z. Phys.* **1927**, *44*, 455.
(5) Roothaan, C. C. J. *Rev. Mod. Phys.* **1951**, *23*, 69.
(6) Roothaan, C. C. J. *Rev. Mod. Phys.* **1960**, *32*, 179.
(7) Hartree, D. R. *Proc. R. Soc. London, Ser. A* **1933**, *141*, 269, and references cited therein.
(8) Fock, V. *Z. Phys.* **1930**, *62*, 795.
(9) Hartree, D. R.; Hartree, W.; Swirles, B. *Philos. Trans. R. Soc. London, Ser. A* **1939**, *299*, 238.
(10) Pauling, L. *J. Am. Chem. Soc.* **1931**, *53*, 1357.
(11) Slater, J. C. *Phys. Rev.* **1932**, *33*, 255.
(12) Wheland, G. W. *Resonance in Organic Chemistry*; Wiley: New York, 1955; and references cited therein.
(13) Bobrowic, F. B.; Goddard, W. A. In *Methods of Electronic Structure Theory*; Shafer, H. F., III, Ed.; Plenum: New York, 1977; p 79.
(14) Cooper, D. L.; Gerrat, J.; Raimondi, M. In *Valence Bond Theory and Chemical Structure*, Klein, D. J., Trinajstic, N., Eds.; Elsevier: Amsterdam, 1990; p 287.
(15) Gerrat, J.; Raimondi, M. *Proc. R. Soc. London, Ser. A* **1980**, *371*, 525.
(16) Møller, C.; Plesset, M. S. *Phys. Rev.* **1934**, *46*, 618.
(17) Paldus, J. In *Theory and Applications of Computational Chemistry: The First 40 Years*; Dykstra, C. E., Frenking, G., Kim, K. S., Scuseria, G. E., Eds.; Elsevier: Amsterdam, 2005; Chapter 7, p 115.
(18) Bartlett, R. J. In *Theory and Applications of Computational Chemistry: The First 40 Years*; Dykstra, C. E., Frenking, G., Kim, K. S., Scuseria, G. E., Eds.; Elsevier: Amsterdam, 2005; Chapter 42, p 1191.
(19) Andersson, K.; Malmqvist, P. A.; Roos, B. O. *J. Chem. Phys.* **1992**, *96*, 1218.
(20) *Fundamental Work of Quantum Chemistry*; Brändas, E. J., Kryachko, E. S., Eds.; Kluwer Academic: Boston, 2003.
(21) *Theory and Applications of Computational Chemistry: The First 40 Years*, Dykstra, C. E., Frenking, G., Kim, K. S., Scuseria, G. E., Eds.; Elsevier: Amsterdam, 2005.
(22) Clementi, E. *Proc. Nat. Acad. Sci. U.S.A.* **1972**, *69*, 2942.
(23) Kryachko, E. S.; Ludeña, E. V. *Energy Density Functional Theory of Many-Electron Systems*; Kluwer Academic: London, 1990.
(24) Parr, R. G.; Yang, W. *Density Functional Theory of Atoms and Molecules*; Oxford University Press: Oxford, U.K., 1985.

(25) Allinger, N.-L.; Ghen, K. S.; Lii, J. H. *J. Comput. Chem.* **1996**, *17*, 642.
(26) Wigner, E. *Phy. Rev.* **1934**, *46*, 1002.
(27) Löwdin, P.-O. *Adv. Chem. Phys.* **1959**, *2*, 207.
(28) Hylleraas, E. A. *Z. Phys.* **1928**, *48*, 469.
(29) Corongiu, G. *Int. J Quantum Chem*. **2005**, *105*, 831.
(30) Shavitt, I. *Methods of Computational Physics*; Academic Press: New York, 1963; Vol. II.
(31) Helgaker, T.; Jensen, H. Ja. Aa.; Jørgensen, P.; Olsen, J.; Ruud, K.; Ågren, H.; Anderson, T.; Bak, K. L.; Bakken, V.; Christiansen, O.; Dahle, P.; Dalskov, E. K.; Enevoldsen, T.; Fernandez, B.; Heiberg, H.; Hettema, H.; Jonsson, D.; Kirpekar, S.; Kobayashi, R.; Koch, H.; Mikkelsen, K. V.; Norman, P.; Packer, M. J.; Saue, T.; Taylor, P. R.; Vahtras O. *DALTON, an ab Initio Electronic Structure Program*, Release 1.0; Oslo, Norway, 1997.
(32) Clementi, E. *J. Chem. Phys*. **1962**, *36*, 33.
(33) Pauncz, R. *The Symmetric Group in Quantum Chemistry*; CRC Press: Boca Raton, FL, 1995.
(34) Löwdin, P.-O. *Phys. Rev.* **1955**, *97*, 1474.
(35) Prosser, F.; Hagstrom, S. *J. Chem. Phys.* **1968**, *48*, 4807.
(36) Linpack Fortran Subroutines Library, available from http://www.netlib.org.
(37) Hiberty, P. C.; Humbel, S.; Byrman, C. P.; van Lenthe. J. H. *J. Chem. Phys*. **1994**, *101*, 5969.
(38) Clementi, E.; Corongiu, G. *Int. J. Quantum Chem*. **2005**, *105*, 709.
(39) Lie, G. C.; Clementi, E. *J. Chem. Phys* **1974**, *60*, 1275.
(40) Lie, G. C.; Clementi, E. *J. Chem. Phys*. **1974**, *60*, 1288.
(41) Sinanoglu, O. *J. Chem. Phys*. **1962**, *36*, 706.
(42) Sinanoglu, O. *Adv. Chem. Phys.* **1969**, *6*, 315.
(43) Siegbahn, P. E. M. In *Methods in Computational Physics*; Dierksen, G. H. F., Wilson, S., Eds.; Reidel: Dordrecht, The Netherlands, 1983; p 189.
(44) Cioslowski, J. *Phys. Rev. A* **1991**, *43*, 1223.
(45) Knowles, P.; Schütz, M.; Werner, H.-J. *Modern Methods and Algorithms of Quantum Chemistry*, Vol. 3; von Newmann: Jülich, Germany, 2000; p 97.
(46) Veillard, A.; Clementi, E. *J. Chem. Phys*. **1969**, *44*, 3050.
(47) Huber, K. P.; Herzberg, G. *Molecular Spectra and Molecular Structure IV. Constants of Diatomic Molecules*. Van Nostrand Reinhold: New York, 1979.
(48) Kołos, W.; Szalewicz, K.; Monkhorst, H. J. *J. Chem. Phys*. **1986**, *84*, 3278.
(49) Gengenbach, R.; Hahn, Ch.; Toennies, J. P. *Phys. Rev. A* **1973**, *7*, 98.
(50) Colin, R.; Dreze, C.; Steinhauer, M. *Can. J. Phys*. **1983**, *61*, 641.
(51) Persico, M. *Mol. Phys.* **1994**, *81*, 1463.
(52) Hofzumahus, A.; Stuhl, F. *J. Chem. Phys*. **1985**, *82*, 5519.
(53) Zemke, W. T.; Stwalley, W. C.; Coxon, J. A.; Hajigeorgiou, P. G. *Chem. Phys. Lett.* **1991**, *177*, 412.
(54) Chakravorty, S. J.; Davidson, E. R. *J. Phys. Chem*. **1996**, *100*, 6167.
(55) Fisher, C. F. *Comput. Phys. Comm*. **1991**, *64*, 369, and references cited therein.
(56) Clementi, E.; Roetti, C. *Roothaan-Hartree−Fock Wavefunctions*; Special Issue of Atomic Data and Nuclear Data Tables; Academic Press: New York, 1974.
(57) **)** Mohanty, A. K.; Parpia, F. A.; Clementi, E. In *Kinetically Balanced Geometric Gaussian Basis Set for Relativistic Many-Electron Atoms, MOTECC-91*; Clementi, E., Ed.; ESCOM: Leiden, The Netherlands, 1991; Chapter 4, p 177.
(58) Pisani, L.; Clementi, E. *J. Chem. Phys*. **1995**, *103*, 9321, and references cited therein.
(59) Fritsche, L. *Phys. Rev. B* **1986**, *33*, 3976.
(60) Valderrama, E.; Ludena, E. V.; Hinze, J. *J. Chem. Phys*. **1999**, *110*, 2343, and reference cited therein.
(61) Lüchow, A.; Anderson, U. J. B. *J. Chem. Phys*. **1996**, *105*, 7573, and references cited therein.
(62) Bhattacharya, A.; Anderson, U. J. B. *Phys. Rev. A* **1994**, *49*, 2441.
(63) Handy, N. C.; Harrison, R. J.; Knowles, P. J.; Schaefer, H. F., III. *J. Phys. Chem*. **1984**, *88*, 4872.
(64) Cencek, W.; Rychlewski, J. *J. Chem. Phys*. **1993**, *98*, 1252.
(65) Stwalley, W. C.; Zemke, W. T. *J. Phys. Chem. Ref. Data* **1993**, *22*, 87.
(66) Moore, C. E. *Atomic Energy Levels*; National Bureau of Standards, Circular 467; NBS: Washington, D.C., 1949.
(67) Stehn, J. R. *J. Chem. Phys*. **1937**, *5*, 186.
(68) Mulliken, R. S. *Int. J. Quantum Chem*. **1971**, *5S*, 83. This reference is reported incorrectly in much of the quantum chemistry literature.
(69) Bender, C. F.; Davidson, E. R. *Phys. Rev.* **1969**, *183*, 23.
(70) Bagus, P. S.; Moser, C. M.; Goethals, P.; Verhagen, G. J. *Chem. Phys*. **1973**, *58*, 1886.
(71) Cooper, D. L. *J. Chem. Phys*. **1984**, *80*, 1961.
(72) Martinazzo, R.; Famulari, A.; Raimondi, M.; Bodo, E.; Gianturco, F. A. *J. Chem. Phys*. **2001**, *115*, 2917.
(73) Fülscher, M. P.; Serrano-Andrés, L. *Mol. Phys*. **2002**, *100*, 903.
(74) Bagus, P. S.; Broer, R.; Parmigiani, F. *Chem. Phys. Lett.* **2006**, *421*, 148.
(75) Clementi, E. *J. Chem. Phys*. **1963**, *38*, 2248.
(76) *Handbook of Chemistry and Physics*, 76th ed.; Lide, D. R., Ed.; CRC: Boca Raton, FL, 1995−1996.
(77) Thomson, R.; Dalby, F. W. *Can. J. Phys*. **1969**, *47*, 1155.
(78) Phelps, P. H.; Dalby, F. W. *Phys. Rev. Lett.* **1966**, *16*, 3.